7-2022

Associating infection by Chlamydia pneumoniae and the presence of amyloid-β plaques in the brains of Alzheimer's disease/ dementia patients

Paul J. G. Carango
Philadelphia College of Osteopathic Medicine

Philadelphia College of Osteopathic Medicine

School of Health Sciences

Graduate Program in Biomedical Sciences

Associating infection by *Chlamydia pneumoniae* and the presence of amyloid-β plaques in the brains of Alzheimer's disease/dementia patients

A Thesis in Biomedical Sciences by Paul J. G. Carango

Submitted in Partial Fulfillment of the Requirements for the Degree of

Master of Science in Biomedical Sciences

July 2022

We, the undersigned, duly appointed committee have read and examined this manuscript and certify it is adequate in scope and quality as a thesis for this master's degree. We approve the content of the thesis to be submitted for processing and acceptance.

Denah M. Appelt, PhD. — 7/26/2022

Dr. Denah Appelt, Thesis Advisor
Professor of Neuroscience
Dept. of Bio-Medical Sciences

Date

Brian Balin, PhD — 7/26/2022

Dr. Brian Balin, Thesis Committee Member
Professor of Neuroscience and Neuropathology
Dept. of Bio-Medical Sciences

Date

Christopher Little — 7/28/2022

Dr. Scott Little, Thesis Committee Member
Associate Professor of Microbiology and Immunology
Dept. of Bio-Medical Sciences

Date

ABSTRACT

Sporadic late-onset AD (LOAD) is the most common form of dementia (Woods et al, 2020). In recent years, significant attention has been given to the role of infection in the pathogenesis of late-onset AD/dementia. The *Cpn* pathogen has been an organism of particular focus following the seminal study Balin et. al 1998 which found that *Cpn* DNA was present in 90% of brains from patients diagnosed with LOAD. Subsequent immunohistochemical studies demonstrated that *Cpn* antigens were present in the frontal and temporal cortices of LOAD brains and that Aβ amyloid plaques found in those regions of the brain co-localize with areas of *Cpn* immunoreactivity (Hammond et al 2010).

This study aims to quantitate *Chlamydia pneumoniae* (*Cpn*) antigen(s) and Aβ amyloid plaques throughout the limbic system and cortical areas of brains from individuals diagnosed with late-onset Alzheimer's disease (AD)/dementia and from individuals diagnosed with non-demented conditions. It was expected that the load of *Cpn* will positively correlate with the load of amyloid plaques in the brains investigated. Furthermore, as it is well established that amyloid plaques are a hallmark of Alzheimer's disease pathology, it is assumed that the load of amyloid plaques and *Cpn* inclusions will be greater in the brains of individuals diagnosed with AD/dementia compared to the load of amyloid plaques and *Cpn* inclusions in brains from individuals not diagnosed with AD/dementia.

Sections of the hippocampus and the prefrontal cortex were dissected and processed for immunostaining from the eight cadaver brains that had been donated to the Pennsylvania Human Gifts Registry. The brains selected included an equal number of

brains with confirmed dementia/AD and brains with no diagnosis of AD/dementia. AD/dementia or non-AD/dementia status was determined based on the listed cause of death (COD. Five sections from the hippocampus and the prefrontal cortex were immunolabeled with specific antibodies for amyloid plaques and *Cpn* and then digitally imaged at 40X. The *Cpn* inclusions and amyloid plaques were counted in each region and normalized using the equivalent total area/section. The data was recorded as mean counts per brain section. The AD/dementia brains showed a load of 1854.00±210.31 amyloid plaques and a load of 2272.75±395.72 *Cpn* inclusions in the hippocampus. The AD/dementia prefrontal cortex displayed a load of 3793.75±997.02 amyloid plaques and a load of 1833.25±470.02 *Cpn* inclusions The non-AD/dementia brains showed a load of 263.00±223.06 amyloid plaques and a load of 332.00±220.30 *Cpn* inclusions in the hippocampus. The non-AD/dementia prefrontal cortex displayed a load of 970.25±636.08 amyloid plaques and a load of 424.75±324.22 *Cpn* inclusions.

This preliminary study yielded data of an association between amyloid pathology and infection by *Cpn* in both AD/demented and non-AD/dementia brains. It was revealed that the load of *Cpn* does correlate with the load of amyloid plaques in all brains where amyloid plaque pathology was present. Furthermore, the load of amyloid plaques and *Cpn* inclusions were substantially greater in brains with an AD/dementia diagnosis compared to brains without and AD/dementia diagnosis. These data help to support prior work demonstrating a relationship between infection and LOAD pathology. Furthermore, this study demonstrated that the Human Gifts registry is a viable and valuable resource of tissue for research purposes.

TABLE OF CONTENTS

LIST OF FIGURES

LIST OF TABLES

ACKNOWLEDGEMENTS

I would like to express my sincerest gratitude to my thesis advisor Dr. Denah Appelt for taking me under her wing and guiding me to this point. The task was surely monumental.

I would also like to thank my thesis committee including Dr. Brian Balin and Dr. Scott Little for their input, expertise, and for laying the groundwork for this project over their years of dedicated research.

And finally I would like to thank the research and support staff at PCOM, including Jacquelyn Gerhart and Mark Martin of the Bio-imaging department, John Pentecost of the IT department, and Dr. Marcus Bell for his consultations on the analysis and presentation of the data.

INTRODUCTION

1.1 Alzheimer's Disease

Alzheimer's disease (AD) is the most common form of dementia, affecting nearly 55 million individuals worldwide. This number is projected to double every 20 years due to the global trend of population aging. According to a 2017 estimate, by 2050 the worldwide incidence of AD is projected to reach 139 million individuals, representing 2.5 times increase in global cases (Guerchet et al, 2020). Furthermore, there is currently no cure or reliable prevention measures for AD. Several prescription drugs are available for symptom management of AD, largely acetylcholinesterase inhibitors, but these drugs only affect a modest improvement in cognition and do not slow disease progression or delay disease onset (Cummings, 2021). Thus, AD represents a major social, health, and economic burden to the caretakers and society.

AD is classified into two main types: early onset AD (EOAD) and late onset AD (LOAD). The two subtypes can be immediately distinguished by age of onset, with the first symptoms of EOAD occurring before the age of 65 and the first symptoms of LOAD occurring after the age of 65 (Bertram et al, 2010; Goate & Hardy, 2012). EOAD and LOAD can be further categorized by what is understood of their underlying causes. EOAD, is familial and thus largely genetic in origin (Bertram et al, 2010). EOAD has been strongly linked to mutations in the genes APP, PSEN1, and PSEN2, which code for amyloid precursor protein (APP), presenilin 1 (PSEN1), and presenilin 2 (PSEN2) respectively (Gonneaud et al, 2021). Additionally, EOAD accounts for ~5% of all AD cases. In contrast LOAD, which makes up the remaining of ~95% of AD cases, is not associated with any specific mutations or conditions and it is thus not currently possible to predict LOAD development with any appreciable degree of certainty (Goate & Hardy,

2012; Gonneaud et al, 2021). LOAD has been associated with a variety of risk factors such as age (Guerrero et al, 2021), a family history of LOAD (Gonneaud et al, 2021), expression of Apolipoprotein E4 (Gerard, 2007; Gonneaud, 2021), quality of diet, amount of physical activity, and presence of healthy social relationships (Parker & Rhee, 2021). The development of LOAD is therefore conceptualized as the result of the complex interactions of several genetic and environmental factors. Despite the differences in the presentation and likely cause, both EOAD and LOAD express the same neuropathological characteristics. These characteristics include the presence of extracellular deposits of amyloid-β (Aβ) plaques and intracellular deposits of neurofibrillary tangles (NFTs) in cortical neurons (Woods et al, 2020).

1.2 Amyloid Precursor Protein and Aβ-Plaque Formation

Aβ plaques are composed of aggregated species of Aβ peptides. These peptides are derived from the sequential enzymatic breakdown of amyloid precursor protein (APP) (Tan et al. 2009). APP is a large type 1 transmembrane protein that is highly expressed in the brain. APP, along with amyloid precursor like protein 1 (APLP1) and amyloid precursor like protein 2 (APLP2), form the mammalian APP gene family. These amyloid precursor proteins form a group of phylogenetically ancient and highly conserved proteins which have important physiological roles in the CNS and PNS. The role of these proteins is not currently defined, but the APP family is associated with nervous system development, the formation and function of the neuromuscular junction, synaptogenesis, dendritic complexity and spine density, axonal growth and guidance, and synaptic functions, including synaptic plasticity, learning and memory (Muller et al, 2017).

APP is notable among this group as it is the only APP gene family protein which contains the Aβ peptide sequence necessary for the formation of Aβ plaques (Muller et al,

2017; Guo et al, 2020). Enzymatic processing of APP can be categorized into two pathways; amyloidogenic and non-amyloidogenic (Wilkins & Swerdlow, 2017; Wilquet & De Strooper, 2004). The non-amyloidogenic pathway is initiated by the action of the α-secretase A-disintegrin and metalloproteinase domain-containing protein 10 (ADAM10). ADAM10 cleaves APP in the ectodomain at a site within the Aβ peptide sequence, thus splitting Aβ between two APP fragments. The first fragment is a soluble peptide sAPPα, which is shed into the extracellular (EC) space, and the second fragment is a carboxy terminal fragment α-Carboxy terminal fragment (α-CTF) which remains embedded in the cell membrane. α-CTF is further cleaved by γ-secretase, a multiprotein complex composed of either Presenilin 1 (PSEN1) or Presenilin 2 (PSEN2), which is the catalytic unit of the protease, nicastrin (NCSTN), anterior pharynx defensive phenotype 1 (Aph-1), and presenilin enhancer-2 (PEN2). Cleavage of α-CTF by γ-secretase results in production of APP intracellular domain (AICD), which is released into the cytoplasm, and the p3 peptide, a non-toxic form of amyloid which is shed into the EC space. The majority of human APP processing occurs down the non-amyloidogenic pathway (Wilkins & Swerdlow, 2017; Steiner et al, 2018; O'Brien et al, 2011).

The amyloidogenic pathway is initiated by the action of the β-secretase beta-site APP cleaving enzyme 1 (BACE1). Like ADAM10, BACE1 cleaves APP in the ectodomain splitting APP into two fragments, sAPPβ, a soluble peptide which is shed into the EC space, and β-CTF, which remains embedded into the cell membrane. However, unlike ADAM10, BACE1 cleaves APP at the amino terminus of the Aβ peptide rather than within the peptide itself. Thus, the resulting membrane embedded β-CTF fragment contains a complete Aβ peptide sequence. β-CTF is then cleaved by γ-secretase producing AICD which, as in the non-amyloidogenic pathway, is released into

the cytoplasm and the Aβ peptide which is released into the EC space (Al-Atrache at al, 2019; Wilkins & Swerdlow, 2017; Steiner et al, 2018; O'Brien et al, 2011). The Aβ peptides produced by γ-secretase processing range from 37 to 43 amino acid residues in length, with Aβ40 accounting for the vast majority of peptides produced followed distantly by Aβ42. The remaining possible Aβ peptide lengths occur only in relatively small amounts. This variance in Aβ peptide length occurs as γ-secretase processes β-CTF in sequential tripeptide-releasing cleavages which may begin at several possible points on the protein. The first cut in the process is referred to as the ε-cleavage, followed by the ζ-cleavage, and finally the γ-cleavage, although not all Aβ peptides require three cuts. The cleavage sites are further defined by reference to the amino acid residue where the cut occurs. For example, in the generation of Aβ40 the first cut occurs at residue 49, followed by residue 46, and finally residue 43. Thus, the pathway would be completely defined as ε-49, ζ-46 and ɣ-43. Aβ42 is generated through the pathway ε-48 and ζ-45 (Steiner et al 2018; Qiu et al, 2015).

Although Aβ40 constitutes the vast majority of species produced by the amyloidogenic pathway, Aβ42 is primarily responsible for the formation of amyloid plaques in AD. The monomeric form of Aβ42 initially produced by the proteolytic breakdown of APP is not known to be cytotoxic or otherwise disruptive to neuronal functioning and may in fact play a role in normal physiological processes. Issues arise, however, if the Aβ42 that accumulates in the neuropil misfolds (Zhou et al, 2012, Verman, 2015). Many factors have been identified as possible triggers for misfolding, such as oxidative stress, glycation, and mutation, but no specific factor or combination of factors has been directly implicated. Misfolded Aβ42 monomers are capable of aggregating into oligomers. These oligomers may organize into protofibrils and

eventually into mature fibrils. Once a critical concentration of mature Aβ42 fibrils has been reached a secondary nucleation reaction occurs. In this reaction, the mature fibrils act as a template and catalyst for the formation of additional oligomers from misfolded Aβ42. Thus, a positive feedback loop is created in which oligomers organize into fibrils which then promote the formation of more oligomers. Both the mature fibrils and the oligomers are known to exert a cytotoxic effect, however the Aβ42 oligomers are considered to be the major driver of neurotoxic damage in AD (Tamango et al 2018; Verma et al, 2015). Ex vivo studies of Aβ42 oligomers have shown that it may trigger invagination and pore formation in the lipid bilayer, dysregulation of calcium homeostasis, stimulation of an inflammatory response, induction of oxidative stress through the formation of metal-Aβ42 complexes, depress synaptic transmission through interference of glutaminergic receptors, induction of apoptosis through the impairment of autophagy mechanisms, and competitively bind to cell surface receptors (Zhao et al, 2012; Mucke & Selkoe, 2012; Tamagno et al; 2018; Verma et al, 2015).

1.3 Neurofibrillary Tangles (NFTs)

NFTs are aggregates of hyperphosphorylated tau. Tau is a highly soluble and intrinsically disordered microtubule-associated protein (MAP) that is found mainly in neurons. Like all MAPs, tau is associated with the formation and stabilization of neuronal microtubule networks as well as the regulation of axon growth (Barage & Sonawane, 2015; Wegmann et al, 2021). Tau is composed of 4 domains: the N-terminal domain, the proline rich domain, the microtubule binding domain, and the C-terminal domain. Due to alternative splicing, primarily within the N-terminal and microtubule binding domains, several isoforms of tau exist. Six of the isoforms are found specifically in the CNS. The six tau isoforms of the CNS are further classified by the number of repeats found within

the microtubule binding domain. Three of the isoforms contain 3 repeating microtubule binding domains and are referred to as 3-repeat (3R) tau while the remaining three isoforms contain 4 repeating microtubule binding domains and are referred to as 4-repeat (4R) tau. The 4R tau has greater microtubule binding affinity than 3R tau due to the additional binding domain repeat (Jouanne et al, 2017; Naseri et al, 2019). These two isoform groups exist in a 1:1 ratio in adult human brains, and disruption of this ratio has been implicated in a variety of tauopathies, including AD.

Tau's affinity to bind to microtubules is regulated through post-translational phosphorylation by the enzymes glycogen synthase kinase 3 (GSK-3β) and cyclin-dependent kinase 5 (cdk5). Specifically, as tau becomes increasingly phosphorylated its affinity for microtubule binding decreases. Tau is normally phosphorylated at specific serine, threonine and tyrosine residues found mostly within the proline rich domain. Under pathological conditions, tau becomes phosphorylated at additional residue sites not indicated in normal tau functioning. Thus, tau that is hyperphosphorylated possesses 3 to 4 times more phosphates per mole than normally functioning tau. In addition to losing the ability to bind to microtubules, hyperphosphorylated tau will polymerize into twisted double stranded fibrils called paired helical filaments (PHFs). It is these PHFs which aggregate to form NFTs (Appelt et al, 1993; Wang J-Z et al, 2013; Jouanne et al, 2017; Morris et al, 2011). The loss of normal tau function and the subsequent formation of NFTs compromises the structural integrity and regulatory functions of the cytoskeleton which results in abnormal cell morphology, compromised axonal transport, disruption of synaptic dysfunction, and ultimately neurodegeneration (Barage & Sonawane, 2015; Wegmann et al, 2021).

1.6 Amyloid Cascade Hypothesis

The amyloid cascade hypothesis has been the predominant theory for describing the pathology of AD for the past few decades (Balin et al, 2018; Garbuz et al, 2020). Under this theory, the neuropathological characteristics of AD may be due to a series of events triggered by the abnormal accumulation of Aβ plaques (Barage & Sonawane, 2015; Balin et al, 2018). For example, it has been demonstrated that Aβ oligomers can trigger the hyper-phosphorylation of tau through activation of neuron surface receptors and thus promote the formation of NFTs (Zhang et al, 2020; Garbuz et al, 2020). Aβ plaque accumulation has also been shown to induce chronic neuroinflammation which can result in neurodegeneration via apoptosis and necrosis of neurons (Carrero et al, 2012; Garbuz et al, 2020). Furthermore, Aβ plaques have been implicated in the disturbance of neural membrane potential, the cholinergic system, an increase in CNS oxidative stress, and the formation of neurites, all of which may further contribute to the neurodegeneration of AD (Barage & Sonawane, 2015; Garbuz et al, 2020).

1.7 Inflammation and LOAD

Neuroinflammation is strongly connected with the development of LOAD pathology (Garbuz et al, 2020; Lee et al, 2008). Neuroinflammation itself is primarily mediated by the action of microglia and astrocytes (Di Sabato et al, 2017). As such, activated microglia and astrocytes are typical characteristics of LOAD pathology (Garbuz et al, 2020). When activated, these cell types release a variety of inflammatory agents, such as pro-inflammatory cytokines, reactive oxygen species, and complement proteins, as a matter of their normal functioning. However, chronic activation of microglia and astrocytes, and by extension chronic exposure to these inflammatory agents, can result in

neuronal damage and cell death typical of neurodegenerative diseases such as AD (Dheen et al, 2007; González-Reyes et al, 2017). For example, it has been demonstrated that mice which have been genetically modified to over produce astrocyte derived IL-6 develop progressive neurodegeneration by 6 months of age (Garbuz et al, 2020). Studies have shown that the probability of developing LOAD correlates with allele variants of genes involved in regulating the immune response (Garbuz et al, 2020; Millington et al, 2014).

There is also evidence that pro-inflammatory cytokines associated with microglia and astrocyte activation may induce an increase in the production of Aβ plaques (González-Reyes et al, 2017). Cytokines IL-1, IL-6, tumor necrosis factor-α (TNF-α) and Transforming growth factor-β (TGF-β) have been implicated in the promotion of APP synthesis and the up regulation of β-secretase, an enzyme partly responsible for the production of Aβ 1-42. (Al-Atrache, 2019; Lee et al, 2008). Additionally, the long-term use of nonsteroidal anti-inflammatory drugs (NSAIDs) have been shown to delay the onset of AD but does not modify LOAD after the manifestation of clinical symptoms. This implicates inflammation as possessing a key role in the initiation of LOAD pathology (Balin et al, 2020; Millington et al, 2014).

1.4 Infection and LOAD

As mentioned previously, the specific etiology of LOAD is unknown. Of particular interest in recent years has been the connection between AD and infection by certain pathogens. Cytomegalovirus (CMV), herpes simplex virus type 1 (HSV1), Borrelia burgdorferi, and *Cpn* have each been implicated in LOAD etiology (Bu et al, 2014; Al-Atrache et al, 2019). CMV DNA has been found in the serum of AD individuals at a significantly higher rate than non-AD individuals (Khodamoradi, 2021). Infection by CMV has also been associated with a two-fold increase in the incidence rate of dementia

(Lee et al, 2019). HSV1 DNA has also been found at a significantly higher rate in the serum of AD individuals (Khodamoradi et al, 2021), as well as within the AD plaques themselves (Wozniak et al, 2008). CNS infection by HSV1 has been shown to disrupt normal glial cell functioning which compromises the homeostatic and immune roles of these cells, and which may promote AD pathology (Mielcarska, 2021). The presence of *B. burgdorferi* IgG has been shown to increase the risk of developing AD (Herrera-Landero et al, 2019). Furthermore, it has been demonstrated that *B. burgdorferi* is present in AD brain tissue via PCR, immunofluorescence, and confocal microscopy and that areas of B. burgdorferi immunoreactivity co-localize with Aβ plaques (Senejani et al, 2021).

Cpn was initially implicated in connection to LOAD etiology in a seminal study by Balin et. al in 1998. It was found that *Cpn* DNA was present in 90% of brain samples taken from patients diagnosed with LOAD. Additionally, the study demonstrated that astrocytes, microglia, and neurons infected with *Cpn* co-localized with areas of AD neuropathology (Balin et al, 1998; Woods et al, 2020). Subsequent studies (Mahoney et al, 2000; Gerard et al, 2006) confirmed the presence of *Cpn* DNA is in brain regions of LOAD patients which exhibit AD neuropathology. Mahoney et al also confirmed the role of microglial cells as reservoirs of *Cpn* infection and thus as potential focal points of AD neuropathology. Additionally, studies have implicated *Chlamydia pneumoniae*'s involvement in promoting the pro-amyloidogenic pathway of APP processing through the upregulation of expression and activity of β-secretase, upregulated expression of γ-secretase, and decreased activity of α-secretase in human astrocytes (Altrache et al, 2019). Other studies have demonstrated a correlation between the presence of *Cpn* in cerebrospinal fluid (Paradowski et al, 2007) and between serum anti-*Cpn* antibodies (Bu

et al, 2015) to AD status. Immunohistochemical have demonstrated that *Cpn* antigens correlate with AD pathology in the frontal and temporal cortices of LOAD patients (Hammond et al, 2010) and in the brains of *Cpn* inoculated mice studies (Little et al, 2004; Little et al, 2014). The mouse studies (Little 2004; Little, 2014) further demonstrated a possible causal role of *Cpn* in Aβ plaque formation. Recently, a robust study from Taiwan utilizing data from the nation's national health service has shown that individuals who have been hospitalized with *Cpn* pneumonia have a significantly higher risk of developing AD (Ou et al, 2021).

The connection between *Cpn* infection and LOAD pathology is currently controversial as several studies seeking to validate or expand upon Balin et al's initial findings failed to find evidence (Balin et al, 2018). Such negative results have been produced from studies regarding PCR analysis (Nochlin et al., 1999; Ring & Lyons, 2000; Taylor et al., 2002; Wozniak et al., 2003), immunohistochemistry (Nochlin et al., 1999; Taylor et al., 2002), and serum anti-*Cpn* antibody detection (Ecemis et al., 2010; Loeb et al., 2004; Yamamoto et al., 2005). However, it should be noted that among the negative studies that sought to replicate aspects of the original study, none used the same methodology as Balin and colleagues (Balin et al, 2018; Woods et al, 2020). Furthermore, many of the studies which show no association are possibly underpowered (Woods et al, 2020).

1.5 *Chlamydia pneumoniae*

Chlamydia pneumoniae (*Cpn*) is a globally ubiquitous obligate intracellular gram-negative bacterium that acts primarily as a pathogen of the respiratory tract (Balin et al, 1998, 2018). Like all species of Chlamydia, *Cpn* has a biphasic life cycle which

alternates between an infectious form and a metabolically active form of the bacterium. The infectious form, referred to as an elementary body (EB), attaches to host cells and promotes entry. Like most intracellular pathogens, *Cpn* EBs form a membrane bound vacuole as they enter the cell. Formation of this vacuole, referred to as a chlamydial inclusion, allows for the creation of an intracellular niche which provides an environment for the replication and release of the bacteria. *Cpn* will remain inside this vacuole for the duration of the intracellular portion of its life cycle (Contini, 2010; Moore, 2014). Once established in the inclusion, the EBs differentiate into the metabolically active form of *Cpn* referred to as the reticulate bodies (RBs). The RBs undergo several rounds of reproduction via binary fission before re-forming into EBs. The EBs are then released via cell lysis, and the process repeats (Balin et al, 2018; Contini et al, 2010). Under normal circumstances, the RBs will multiple and differentiate into EBs over a period of 48-72 hours (Deniset et al, 2010; Kern et al, 2009). Mouse models investigating the course of *Cpn* induced pneumonia demonstrated that live bacteria could be recovered from the lungs up 48 days post infection and lung pathology was recorded to persist up to 60 days post infection (Yang et al, 1993). *Cpn* is however capable of diverting from its normal life cycle under certain conditions. If an RB is exposed to stressful stimuli, such as the presence of penicillin or pro-inflammatory cytokines, the metabolism of the bacteria slows and both replication and differentiation halt. *Cpn* can exist in the body in this state of quiescent for decades resulting in a state of chronic infection referred to as persistence (Balin et al, 2018; Contini et al, 2010).

1.8 *Cpn* as a causative agent of LOAD

As is the case with all chlamydial infections, infection by *Cpn* promotes the secretion of pro-inflammatory cytokines by the immunocompetent cells of the CNS in response to outer membrane proteins, heat shock proteins, and lipopolysaccharides (LPS) (Balin et al, 2018; Contini et al, 2010). LPS is particularly implicated in the inflammation caused by bacterial infection. Experiments using LPS derived from E. coli have been shown to elicit a disproportionately strong inflammatory response (Terrando et al, 2010). Other studies of the effects of LPS initiated neuroinflammation have more directly implicated the molecule in LOAD pathology. LPS injected into the brains of mouse models has been demonstrated to impair memory, promote the production of Aβ 1-42, and enhance expression of genes involved in inflammation and Aβ plaque production (Lee et al, 2008; Gasparini et al, 2004). Infection by *Cpn* itself is associated with an increased expression of enzymes associated with the formation of Aβ 1-42 and stimulation of an inflammatory response (Al-Atrache et al, 2019; Lim et al, 2014). Thus, there exists a clear throughline linking infection by *Cpn* to two well established mediators of LOAD formation and progression; persistent neuroinflammation and Aβ plaque formation.

1.9 Hypothesis and Specific Aims

1.9.1 Hypothesis

Chlamydia pneumoniae has been previously observed throughout the limbic system and cortical regions in diagnosed dementia brains. The working hypothesis underlying these studies is that the load of *Chlamydia pneumoniae* correlates with degree of amyloid pathology and subsequently the severity of dementia.

1.9.2 Specific Aims

In order to define the load of *Chlamydia pneumoniae* relative to the amyloid plaque formation in the limbic system and cortical regions, immunohistochemical analysis will be performed. The brains were selected from individuals who have been diagnosed with dementia and/or Alzheimer's and were compared to normal control brains donated from the Humanity Gifts Registry (HGR).

MATERIALS

Table 2.1: Brains Used in Study

AD/Dementia		
Age	*Cause of Death*	*Gender*
92	Dementia	Female
96	AD, Dementia	Female
84	AD type Dementia	Female
82	Dementia	Male
Non-AD/Dementia		
Age	*Cause of Death*	*Gender*
92	Coronary Artery Disease	Female
94	COPD	Female
87	Cerebral Vascular Disease	Male
86	COPD	Male

Table 2.2: Tissue collected for analysis

Brain Structure	**Tissue Analyzed**	**Area Analyzed**
Anterior Hippocampus	40 tissue sections for amyloid plaques (5 tissue sections per anterior hippocampus x 8 brains) 40 tissue section for *Cpn* inclusions (5 tissue sections per anterior hippocampus x 8 brain)	4.46 mm^2/sections for each of the 5 tissue sections. Total area of 89.2 mm^2 for each brain structure of a given label type
Prefrontal Cortex	40 tissue sections for amyloid plaques (5 tissue sections prefrontal cortex x 8 brains) 40 tissue section for *Cpn* inclusions (5 tissue sections per prefrontal cortex x 8 brains)	4.46 mm^2/sections for each of the 5 tissue sections. Total area of 89.2 mm^2 for each brain structure of a given label type

Table 2.3: Antibodies and kits utilized

Antibody	**Kit**
Synaptic Systems Abeta 42 antibody (Catalog# 218 703) 1:750 dilution	Abcam Mouse and Rabbit Specific HRP/DAB IHC Detection Kit - Micro-polymer (Catalog# ab236466)
Fitzgerald *Chlamydia pneumoniae* antibody (Catalog# 10-C27E) 1:20 dilution	Abcam Mouse and Rabbit Specific HRP/AEC IHC Detection Kit - Micro-polymer (Catalog# ab236467)

METHODS

3.1 Collecting Brain Tissue

A list of Human cadaver brains donated to the Human Gifts Registry (HGR) in Pennsylvania for anatomy lab dissection was compiled with the aim of creating a group of brains with AD/dementia and a group of brains without AD/dementia which were controlled for age and gender. Eight brains were identified which met this criteria, four brains in the AD category and four brains in the non-AD category (Table 2.1). From these brains, areas of the hippocampus and the prefrontal cortex were dissected (Table 2.2). These areas were then processed via an automatic tissue processor, embedded in paraffin, and sectioned.

3.2 Labeling

Serial slides from each brain section were stained for either Aβ plaques or *Cpn*. To prepare the slides for staining, the slides were left on a warmer overnight at 55°C. The slides were deparaffinized automatically in a Gemini Slide Stainer by Thermo Fisher Scientific according to a pre-set lab protocol.

3.3 *Cpn* Staining

Mouse and Rabbit Specific HRP/AEC IHC Detection Kit - Micropolymer (ab236466) and the provided protocol were used (Table 2.3). Hydrogen peroxide block was applied to the slides for 10 minutes. Antigen retrieval was then performed. 10mM citrate buffer solution was heated via microwave until boiling. The slides were placed in the heated citrate buffer solution for 20 minutes. The slides were washed in PBS for 5 minutes. Protein block was applied for 10 minutes. The primary antibody, Fitzgerald *Chlamydia pneumoniae* antibody (10-C27E), was diluted 1:20 in PBS (Table 2.3). The prepared antibody was incubated at room temperature for 2 hours. An unconjugated rabbit anti-mouse antibody, referred to in the kit as mouse complement, was applied for 10 minutes, followed by Goat anti-rabbit HRP conjugate for 30 minutes and finally AEC single solution for 5 minutes. The slides were then counterstained with Mayer's hematoxylin for 45 seconds and rinsed in Richard Allan Scientific bluing reagent (<1.0% <1.0% Sodium bicarbonate, magnesium sulfate, >99%water, <1% 1-Tetradecanaminium, N,N,N-trimethyl-, bromide) for a minimum of 30 seconds and until appropriately blue. The slides were then mounted with an aqueous mounting medium and left to dry overnight.

3.4 Aβ Plaque Staining

Mouse and Rabbit Specific HRP/DAB IHC Detection Kit - Micropolymer (ab236467) and the provided protocol were used (Table 2). Hydrogen peroxide block was applied to the slides for 10 minutes, followed by protein block for 20 minutes. The primary antibody was then prepared. Synaptic Systems Aβ42 antibody (218 703) was diluted 1:750 in PBS (Table 2.3) and left to incubate at room temperature for 2 hours.

Goat anti-rabbit HRP conjugate was applied for 15 minutes. 30µL of DAB chromogen was added to 1500µL of DAB substrate. DAB solution was applied to the slides for 5 minutes. The slides were then counterstained with Mayer's hematoxylin for 45 seconds and rinsed in a bluing solution for a minimum of 30 seconds and until appropriately blue. The slides were then mounted with an aqueous mounting medium and left to dry overnight.

3.5 Quantification

Digital scans of the stained slides were created using a MoticEasyScan Pro set at 40x magnification. The digital scans were opened in Nikon's NIS-Elements AR program. Using the native functions of the program, an appropriate sub-region of the tissue was demarcated by an oval with an area of 4.46mm^2. The shape and area of this demarcation was held constant across all slides used in the experiment, and the specific location of the demarcation was held constant for all hippocampal or pre-frontal tissues slides from a given brain. Within that area, the number of *Cpn* inclusion bodies and Aβ plaques were quantified. Additionally, the dimeters of each of the Aβ plaques were measured. The raw data was then exported from NIS-Elements AR into Microsoft Excel. The ratio of *Cpn* inclusions bodies and Aβ plaques were then calculated. The diameters of the Aβ plaques were organized into three size categories as derived from criteria from Hammond et al 2010.

RESULTS

4.1 Brain Tissue Labeled for Amyloid Plaques and Chlamydial Inclusions

The non-AD brain revealed that the anti-amyloid and anti-*Cpn* labeling of the plaques and inclusions in both the hippocampus and prefrontal cortex were fewer in

number as compared to the AD/Dementia brains (Figure 4.1). The distribution of the amyloid plaques and *Cpn* inclusions are not uniform, however, the majority of the amyloid plaques and *Cpn* inclusions are found in relatively dense clusters separated by large areas of little to no labeling as observed in figure 4.1. In the non-AD brain, the amyloid plaques in the hippocampus are large, fewer in number, and have a dense core appearance (Figure 4.1a) compared to the plaques found in the prefrontal cortex which tend to be smaller more numerous, and diffuse (Figure 4.1c). The morphology of the *Cpn* inclusions in the non-AD/dementia hippocampus (Figure 4.1b) and prefrontal cortex (Figure 4.1d) are similar, with the labeling overall revealing inclusions with well-defined borders. Larger more diffuse *Cpn* inclusions are occasionally found, but they are uncommon and did not appear associated with a specific brain or brain region.

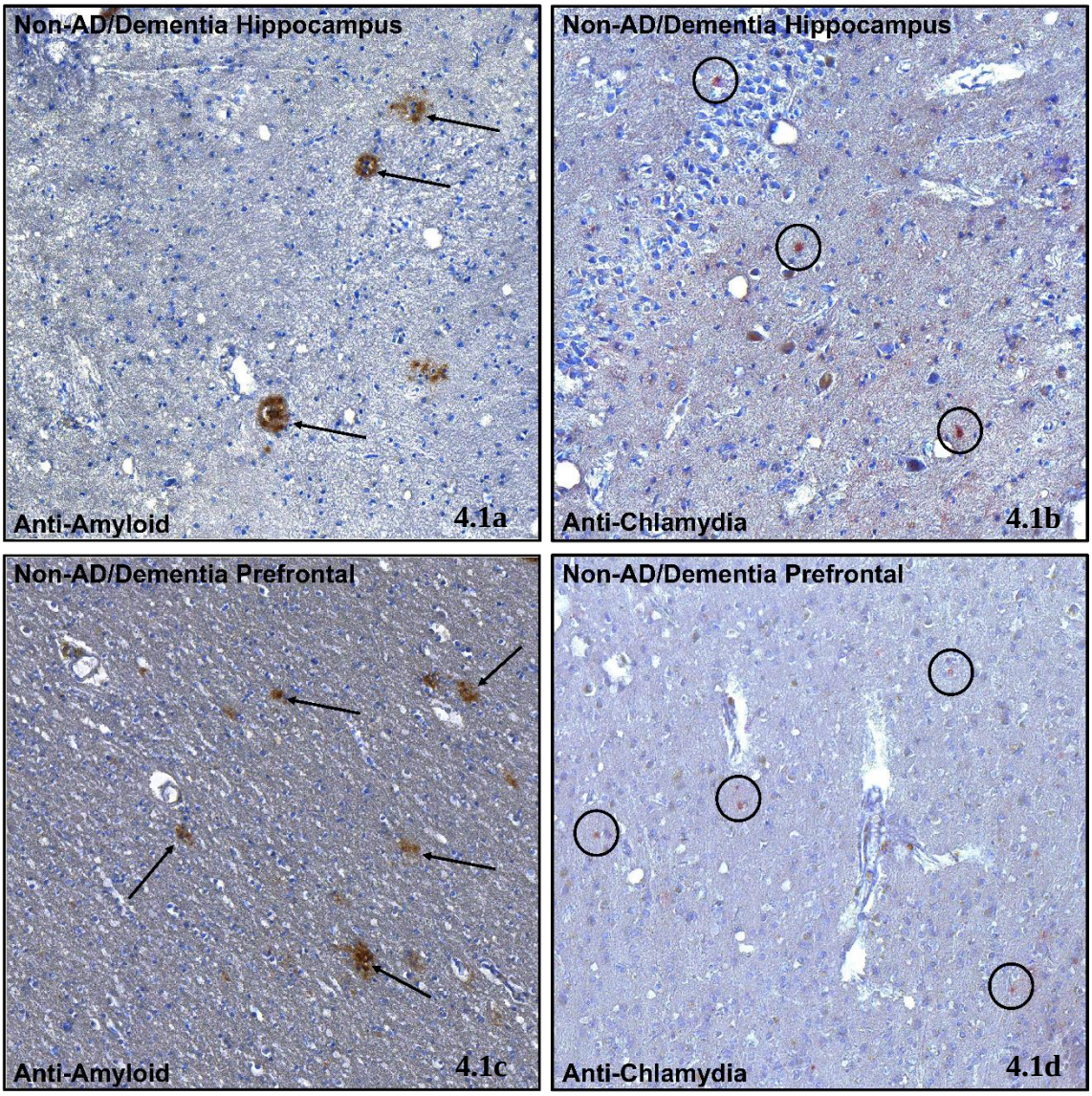

Figure 4.1 Non-AD/dementia tissue from the anterior hippocampus and the prefrontal cortex revealed amyloid plaques in the and Chlamydial inclusions within the same regions.
In both the prefrontal cortex and the hippocampus, the tissues were immunoreacted with antibodies identifying the amyloid plaques (brown reaction) and *Cpn* inclusions (red reaction) 4.1a is a representative image of a non-AD/dementia hippocampus labelled for amyloid plaques, while 4.1b is a representative image of a serial section of the same hippocampus labelled for the presence of *Cpn*. 4.1c is a representative image of a non-AD/dementia prefrontal cortex labelled for amyloid plaques, while 4.1d is a representative image of a serial section of the same prefrontal cortex labelled for the presence of *Cpn*. Images captured at 40x magnification.

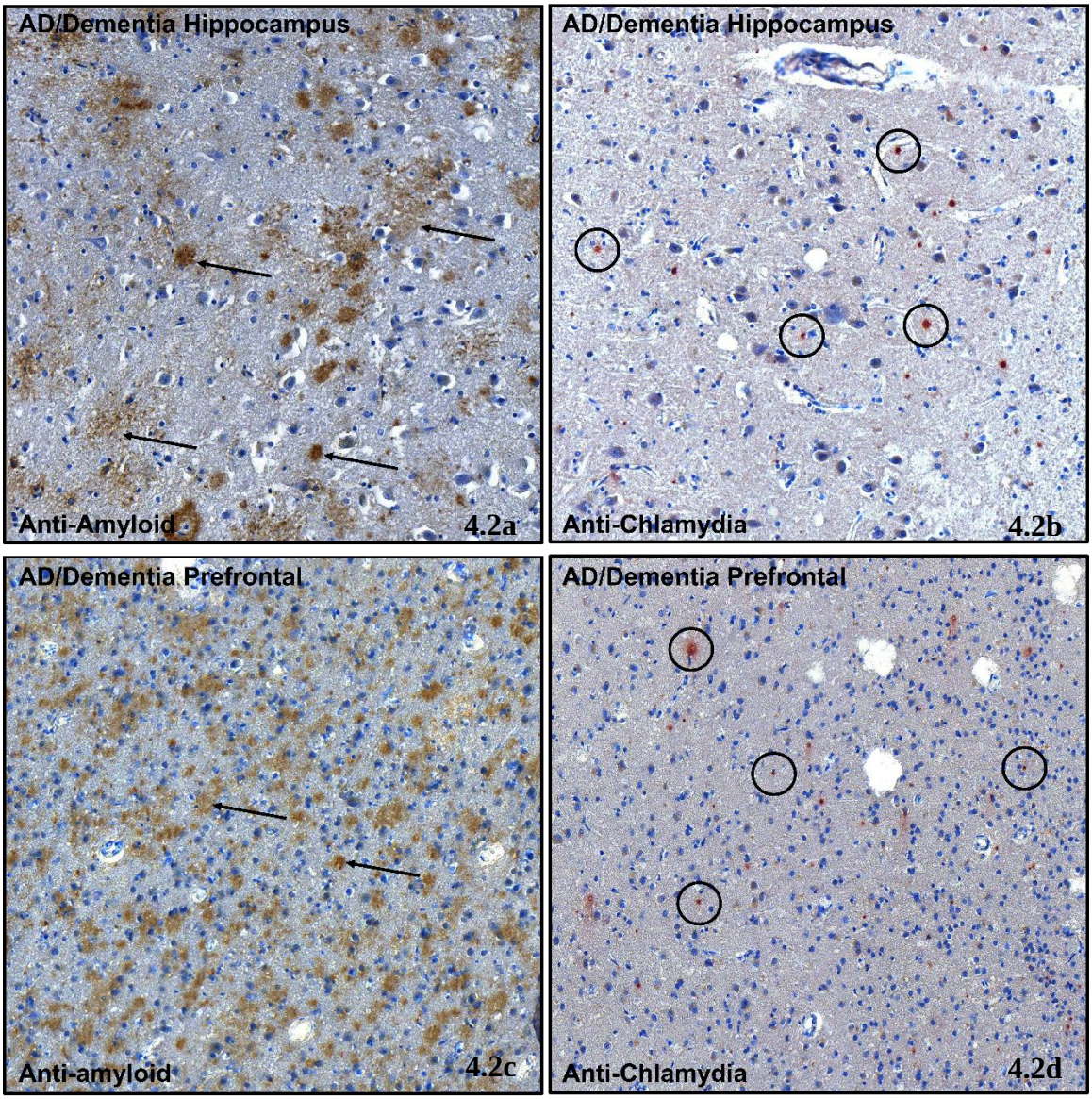

Figure 4.2 AD/dementia brain tissue from the anterior hippocampus and the prefrontal cortex revealed amyloid plaques and Chlamydial inclusions.

In both the prefrontal cortex and the hippocampus, the tissues were immunoreacted with antibodies identifying the amyloid plaques (brown reaction) and *Cpn* inclusions (red reaction) 4.2a is a representative image of an AD/dementia hippocampus labelled for amyloid plaques, while 4.2b is a representative image of a serial section of the same hippocampus labelled for the presence of *Cpn*. 4.2c is a representative image of a AD/dementia prefrontal cortex labelled for amyloid plaques, while 4.2d is a representative image of a serial section of the same prefrontal cortex labelled for the presence of *Cpn*

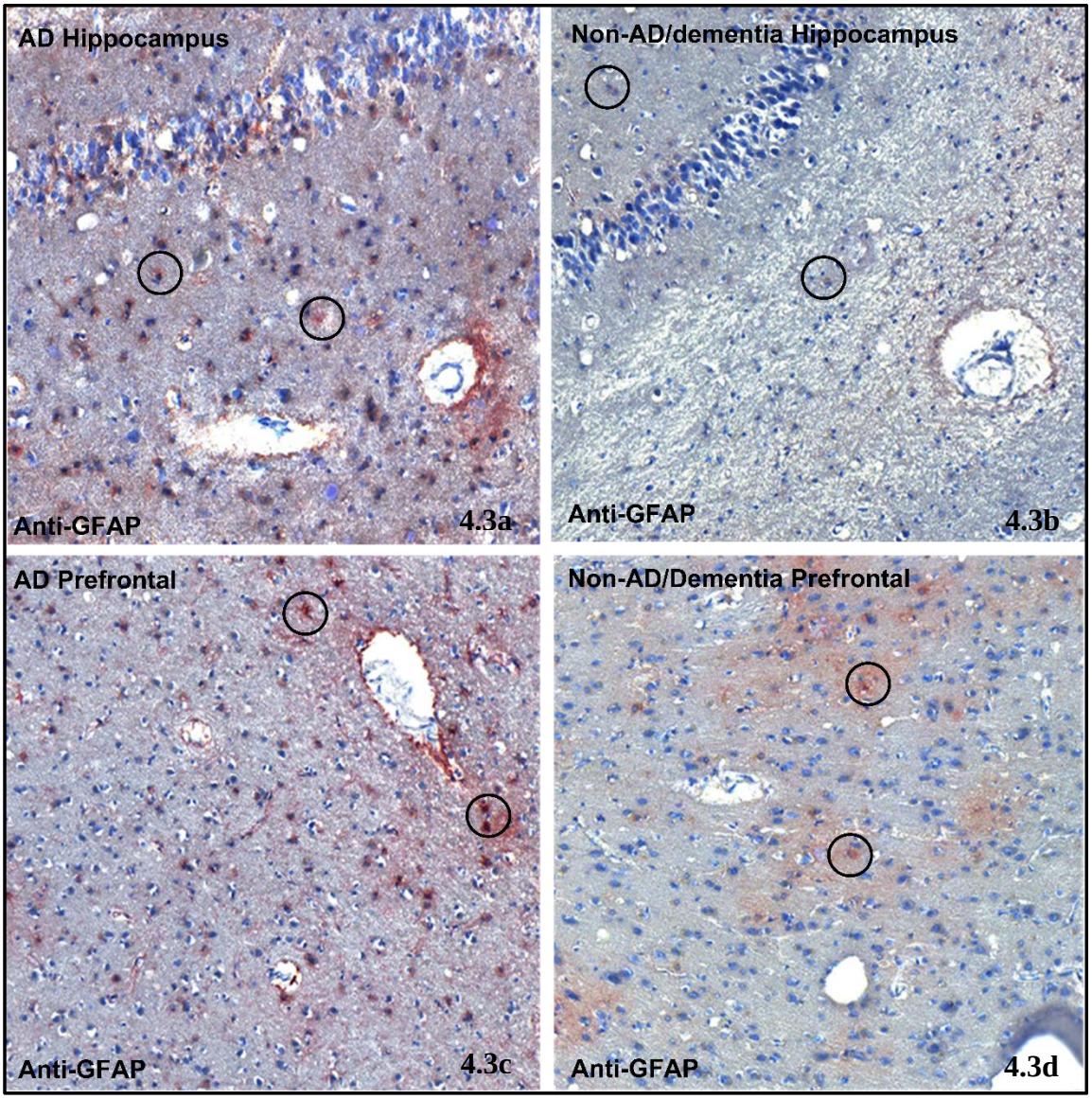

Figure 4.3 Representative micrographs of AD/dementia and non-AD/dementia tissue from the anterior hippocampus and the prefrontal cortex immunolabeled for the presence of GFAP.

Tissue sections of the hippocampus and prefrontal cortex from both AD/dementia and non-AD/dementia brains were labelled for the presence of GFAP (red reaction). 4.3a is a representative image of an AD/dementia hippocampus labelled for GFAP. 4.3b is a representative image presence of a non- AD/dementia hippocampus labelled for GFAP. 4.3c is a representative image of an AD/dementia prefrontal cortex labelled for GFAP. 4.3d is a representative a non-AD/dementia prefrontal cortex labelled for the presence of GFAP.

In the AD/dementia brains (Figure 4.2) The density of amyloid plaques and *Cpn* inclusions is notably greater in the prefrontal cortex than the hippocampus. The amyloid plaques within the prefrontal cortex are discrete and relatively small (Figure 4.2c). The

amyloid plaques within the hippocampus (figure 4.2a) are a mix of highly diffuse cloud-like plaques alongside relatively large plaques with a dense-core appearance. No notable difference exists in the *Cpn* inclusion morphology between the AD/dementia hippocampus (4.2b) and the AD/dementia prefrontal cortex (4.2d). The anti-*Cpn* labeling in both brain regions revealed small *Cpn* inclusions which are uniformly distributed throughout the tissue.

Additionally, the AD/dementia brains and non-AD/dementia brains were immunoreacted with GFAP antibodies to determine the presence of glial cells in association with the amyloid and *Cpn* inclusions in the hippocampus and prefrontal cortex (Figure 4.3). The AD/dementia hippocampus (4.3a) and AD/dementia prefrontal cortex (4.3c) appeared to have a greater amount of GFAP labeling as compared to the non-AD/dementia brain hippocampus (4.3b) and non-AD/dementia prefrontal cortex (4.3d).

4.2 Quantitative Analysis of Amyloid plagues and Chlamydial inclusions

Quantitative analysis was performed to determine the amyloid load in the AD/dementia vs non-AD/dementia brains in the hippocampus and the prefrontal region (Figure 4.4). The amyloid plaque count for the AD/dementia group in the hippocampus was 1854.00±210.31 and prefrontal cortex was 3793.75±997.02. In the non-AD/dementia group the amyloid plaque load in the hippocampus (263.00±223.06) and prefrontal cortex (970.25±636.08) (Figure 4.4). In both the hippocampus and the prefrontal region of the AD/dementia brains, the load of amyloid plaques was greater than in the non-AD/dementia brain. Additionally, the *Cpn* inclusion load in the AD/dementia hippocampus (2272.75±395.72) and prefrontal cortex (1833.25±470.02) were greater

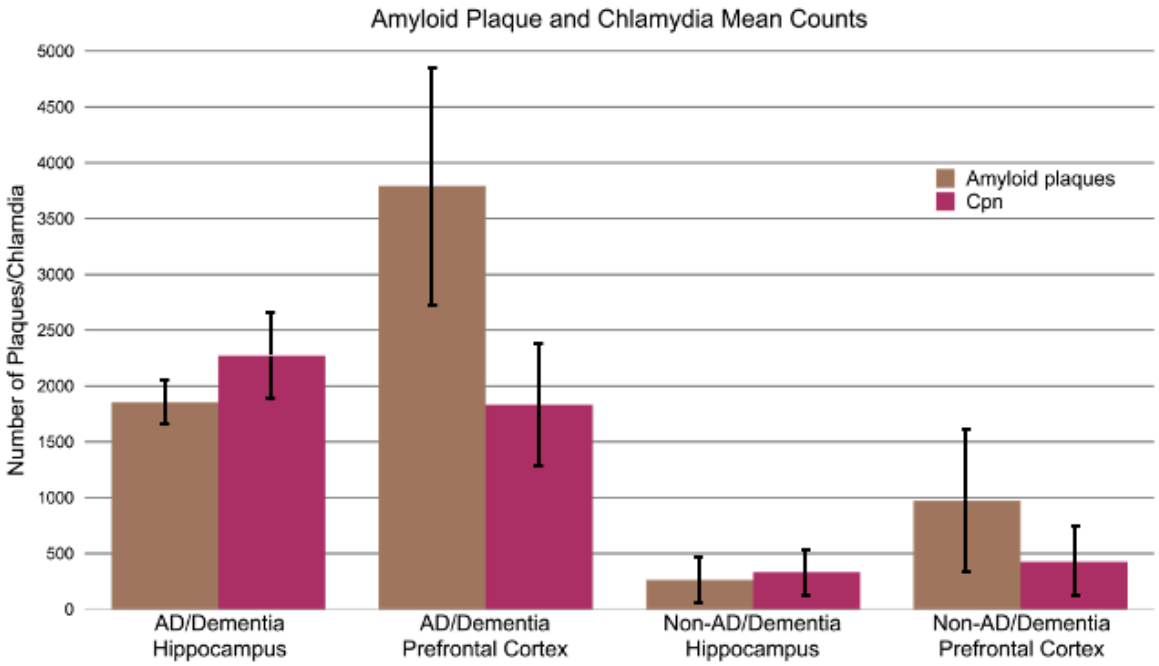

Figure 4.4 Comparison of the total count means of amyloid plaques and *Cpn* inclusions in the hippocampus and prefrontal cortex of AD/dementia and non-AD/dementia brains. The x-axis represents the compiled mean counts of amyloid plaques and Cpn inclusions from the AD/dementia or non-AD/dementia brains as organized by the brain structure examined. While the y-axis represents the mean itself. The brown bars represent the amyloid plaque means counts while the red bars represent the *Cpn* mean counts.

than the *Cpn* inclusion load in the non-AD/dementia hippocampus (332±220.30) and in the prefrontal cortex (424.75±324.22).

Within the AD/dementia brains, the amyloid plaque load of the prefrontal cortex (3793.75±997.02) is greater than the amyloid plaque load of the hippocampus (1854±210.31). This trend also holds true for the non-AD/dementia group, in which the amyloid plaque load of the prefrontal cortex (970.25±636.08) possesses a greater amyloid plaque load than that of the hippocampus (263.00±223.06). The within group trend does not hold true to the load of *Cpn* inclusions, however. Within the AD/dementia brains, the load of *Cpn* inclusions is greater in the hippocampus (2272.75±395.72) than in the prefrontal cortex (1833.25±470.02). Within the non-AD/dementia brains, the number of

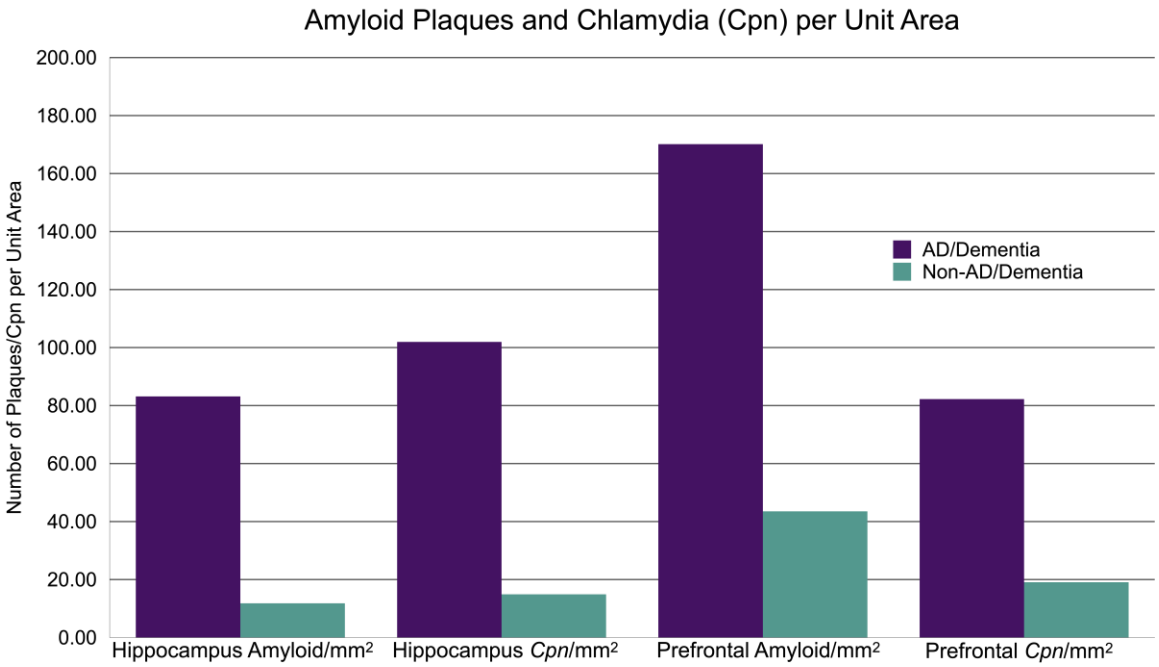

Figure 4.5 Comparison of the density of amyloid plaques and *Cpn* inclusions per mm^2 in the hippocampus and prefrontal cortex of AD/dementia and non-AD/dementia brains. The x-axis represents the amyloid/mm^2 or *Cpn*/mm2 counts for either the hippocampus or prefrontal cortex of the brains investigated. The y-axis represents the number of either amyloid plaques or *Cpn* inclusions per unit area. The purple bars represent the counts from the AD/dementia brains and the green bars represent the counts from the Non-AD/Dementia brains.

Cpn inclusions is greater in the prefrontal cortex (424.75±324.22) than in the hippocampus (332.00±220.30), however there is appreciable overlap in the standard error of the two datasets.

The AD/dementia prefrontal cortex demonstrates a substantially greater load of amyloid plaques (3793.75±997.02) compared to *Cpn* inclusions (1833.00±470.02). The non-AD/dementia prefrontal cortex also demonstrates a significantly greater load of amyloid plaques (970.25±636.08) compared to *Cpn* inclusions (424.75±324.22). In contrast, the AD/dementia hippocampus demonstrates a greater load of *Cpn* inclusions (2272.75±395.72) than amyloid plaques (1854.00±210.31). The amyloid plaque to *Cpn* load difference in the hippocampus is less than the difference observed in either the AD/dementia or non-AD/dementia prefrontal cortex. The non-AD/dementia hippocampus

shows a greater load of *Cpn* inclusions (332.00±220.30) than amyloid plaques (263.00±223.06), however there is major overlap in the standard error between the *Cpn* inclusion load and amyloid plaque load.

The density of amyloid plaque is greater in the AD/dementia hippocampus (83.13/mm^2) and AD/dementia prefrontal cortex (170.12/mm^2) compared to the amyloid plaque density in the non-AD/dementia hippocampus (11.79±10.00/mm^2) and non-AD/dementia prefrontal cortex (43.51/mm^2), respectively (Figure 4.5). Similarly, the *Cpn* inclusion density is greater in the AD/dementia hippocampus (101.92/mm^2) and AD/dementia prefrontal cortex (82.21/mm^2) than the *Cpn* inclusion density in the non-AD/dementia hippocampus (14.89/mm^2) and non-AD/dementia prefrontal cortex (19.05/mm^2).

In addition to total counts and density, the amyloid plaques were further organized into three diameter ranges; 0-24.9 μm, 25-49.9 μm, and 50+ μm. Figure 4.6 shows the frequency of amyloid plaques within each of these categories. As this figure is derived from the same dataset as the total counts, the data follows the amyloid plaque load trend established in figure 4.1. The AD/dementia brains demonstrate a greater amyloid plaque burden than the non-AD/dementia brains in both the hippocampus and prefrontal cortex regions across all three diameter ranges. For the AD/dementia brains, the prefrontal cortex demonstrates a greater amyloid plaque load than the hippocampus in the 0-24.9 μm and 25-49.9 μm categories. The 50+ μm category for both the AD/dementia prefrontal cortex and AD/dementia hippocampus are similar, however. This same trend can be observed within the non-AD/dementia brains as well. The non-AD/dementia prefrontal cortex demonstrates a greater amyloid plaque load than the non-AD/dementia hippocampus in the 0-24.9 μm and 25-49.9 μm categories, while the 50+

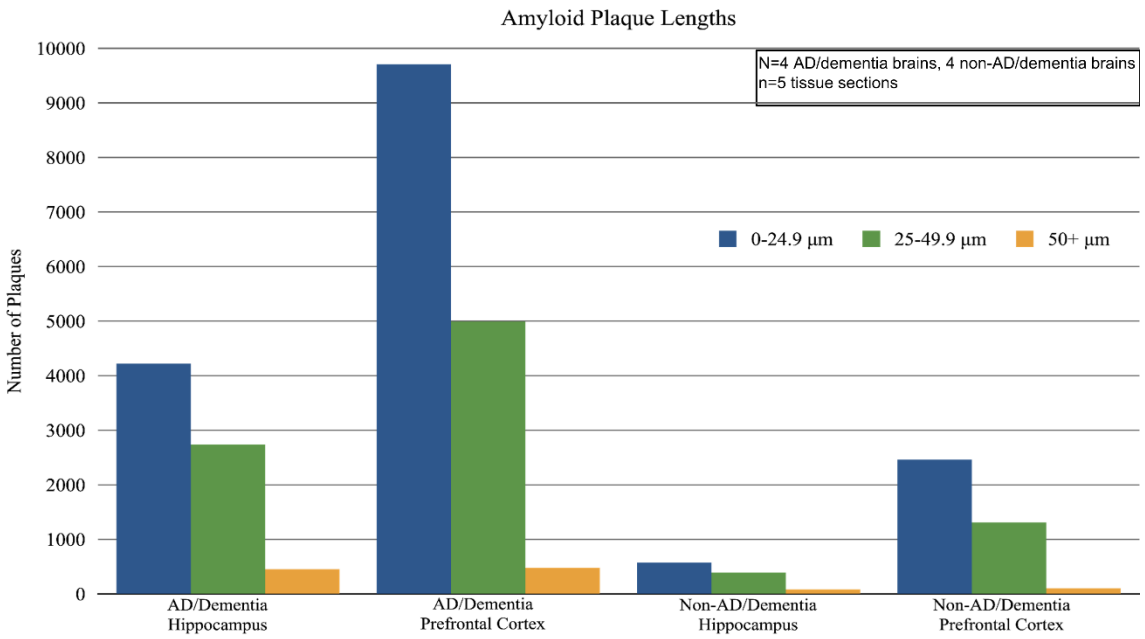

Figure 4.6 Distribution of amyloid plaques across three diameter ranges in the hippocampus and prefrontal cortex of AD/dementia and non-AD/dementia brains.
The x-axis represents the amyloid plaque diameter categories from the AD/dementia and non-AD/dementia brains organized by the brain structure examined. The y-axis represents the total number of plaques within each diameter category. The blue bars represent the number of plaques which fell within a diameter range of 0-24.9 µm, the green bars represent the total plaques which fell into the 25-49.9 µm diameter range, and the yellow bars represent the total number of plaques which fell into the 50+ µm diameter range. These diameter ranges where derived from criteria established by Hammond et al, 2010.

counts are similar. The relative amounts of plaques per diameter category appear consistent across all groups, with the majority of plaques falling within the 0-24.9 µm category, followed by the 25-49.9 µm, and finally the 50+ µm category.

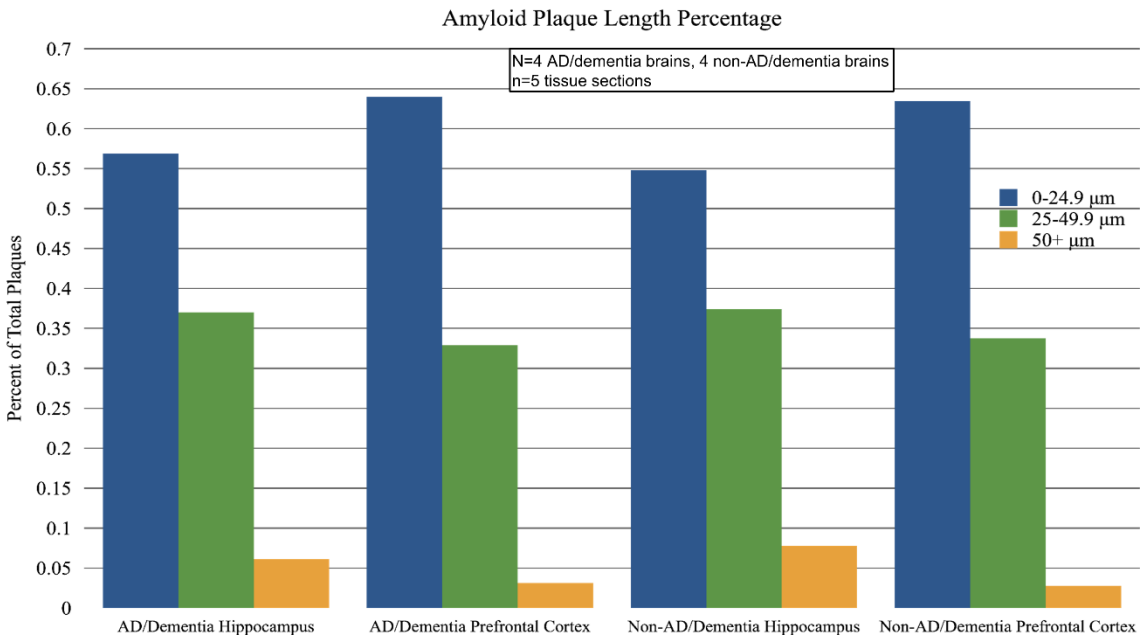

Figure 4.7 Distribution of amyloid plaques across three diameter ranges as a percentage of total plaque load in the hippocampus and prefrontal cortex of AD/dementia and non-AD/dementia brains.
The x-axis represents the total amyloid plaque diameter ranges from the AD/dementia and non-AD/dementia brains organized by the brain structure examined. The y-axis represents the percentage of plaques which make up each of the three diameter ranges. The blue bars represent the percentage of plaques which fell within a diameter range of 0-24.9 µm, the green bars represent the percentage of plaques which fell into the 25-49.9 µm diameter range, and the yellow bars represent the percentage of plaques which fell into the 50+ µm diameter range.

AD/dementia and non-AD/dementia brains, elucidates this trend (Figure 4.7). The 0-24.9 µm diameter category accounts for 57% of the plaques in the AD/dementia hippocampus, 64% of the plaques in the AD/dementia prefrontal cortex, 55% of the non-AD/dementia hippocampus, and 63% of the non-AD/dementia prefrontal cortex. The 25-49.9 µm accounts for 37% of the plaques in the AD/dementia hippocampus, 33% of the plaques in

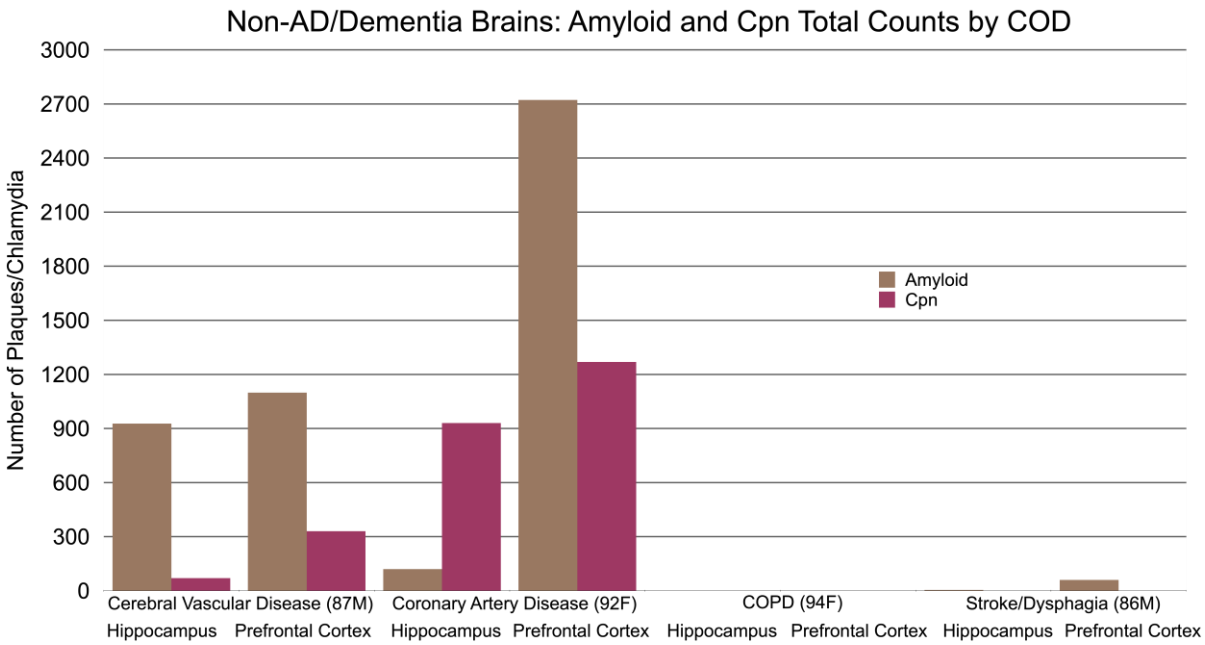

Figure 4.8 Comparison of the amyloid plaque and *Cpn* inclusion in the hippocampus and prefrontal cortex of the non-AD/dementia brains by COD.
The x-axis represents each of the non-AD/dementia brains as identified by the COD provided by the humanity gifts registry. Furthermore, under each COD identifier is a secondary x-axis which identifies a grouping of bars as representing data from either the hippocamus or prefronal cortex of the brain in question. The y-axis represents the number of either amyloid plaques or *Cpn* inclusions. The brown bars represent the amyloid plaque counts while the red bars represent the *Cpn* inclusion counts.

the AD/dementia prefrontal cortex, 37% of the non-AD/dementia hippocampus, and 34% of the non-AD/dementia prefrontal cortex. And finally, the 50+ μm category accounts for accounts for 6% of the plaques in the AD/dementia hippocampus, 3% of the plaques in the AD/dementia prefrontal cortex, 8% of the non-AD/dementia hippocampus, and 3% of the non-AD/dementia prefrontal cortex.

Nearly all the amyloid plaque and *Cpn* inclusion counts for the non-AD/dementia brains were derived from two brains (Figure 4.8). Specifically, the brain with cerebral vascular disease were listed as the cause of death (COD) and the brain with coronary artery disease listed as the COD. For the cerebral vascular disease brain, the load of

amyloid plaques (1099) and the load of *Cpn* inclusions (330) in the prefrontal cortex is greater than the load of amyloid plaques (927) or *Cpn* inclusions (70±54.94) in the hippocampus. For the coronary artery disease brain, the load of amyloid plaques (2722) and the load of *Cpn* inclusions (1269) in the prefrontal cortex is greater than load of amyloid plaques (120) or *Cpn* inclusions (930) in the hippocampus. For the COPD brain, the amyloid plaque and *Cpn* inclusion counts are 0. For the stroke/dysphagia brain, load of amyloid plaques (60) in the prefrontal cortex is greater than the load of amyloid plaques in the hippocampus (5). The *Cpn* inclusion counts for the stroke/dysphagia for both the prefrontal cortex and hippocampus are 0.

The prefrontal cortex of the coronary artery disease brains shows a greater amyloid plaque load (2722) and *Cpn* inclusion load (1269) than amyloid plaque load (1099) or *Cpn* inclusion load (330±6.12) of the prefrontal cortex of the cerebral vascular disease brain. The amyloid plaque load in the hippocampus of the coronary artery disease brain (120) is less than the amyloid plaque load in the hippocampus of the cerebral vascular disease brain (927). The *Cpn* inclusion load (1269) in the hippocampus of the coronary artery disease brain is greater than the *Cpn* inclusion load (70) in the hippocampus of the cerebral vascular disease brain.

Among the AD/dementia brains, the load of amyloid plaque and the load of *Cpn* inclusions does not seem to vary with COD (Figure 4.9). The two brains with AD listed as COD (AD, Dementia; AD Type Dementia) and the two brains with only dementia

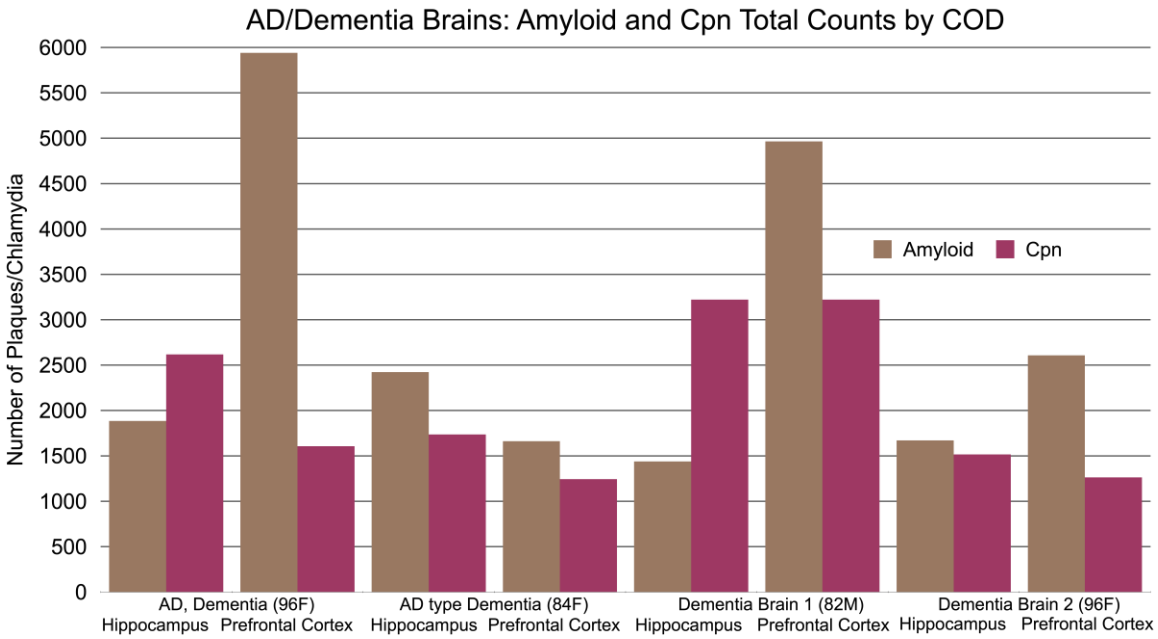

Figure 4.9 Comparison of the amyloid plaque and *Cpn* inclusion loads in the hippocampus and prefrontal cortex of the AD/dementia brains by COD.
The x-axis represents each of the AD/dementia brains as identified by the COD provided by the humanity gifts registry. Furthermore, under each COD identifier is a secondary x-axis which identifies a grouping of bars as representing data from either the hippocamus or prefronal cortex of the brain in question. The y-axis represents the total number of either amyloid plaques or *Cpn* inclusions. The brown bars represent the amyloid plaque counts while the red bars represent the *Cpn* inclusion counts.

listed as COD (Dementia Brain 1; Dementia Brain 2) contributed equally to the total counts. For the AD, dementia brain, the load of amyloid plaques is greater in the prefrontal cortex (5940±38.18) than the load of amyloid plaques in the hippocampus (1884), while the load of *Cpn* inclusions is lesser in the prefrontal cortex (1606) than in the hippocampus (2618). Within the AD dementia hippocampus itself, the load of *Cpn* inclusions (2618) is greater than the load of amyloid plaques (1884). While, within the AD/dementia prefrontal cortex, the load of *Cpn* inclusions (1606) is less than the load of amyloid plaques (5940).

For the AD type dementia brain, the load of amyloid plaques (2423) and *Cpn* inclusions (1736) in the hippocampus is greater than the load of amyloid plaques (1662)

and *Cpn* inclusions (1243) in the prefrontal cortex. Within the AD type dementia brain hippocampus, the load of amyloid plaques (2423) is greater than the load of *Cpn* inclusions (1736). This is also true of the prefrontal cortex within the AD type dementia brain, with the load of amyloid plaques (2423) being greater than the load of *Cpn* inclusions (1243).

For the dementia brain 1, the load of amyloid plaques in the prefrontal cortex (4965) is greater than the load of amyloid plaques in the hippocampus (1439). The load of *Cpn* inclusions in the dementia brain 1 prefrontal cortex (3221) is equal to the load of *Cpn* inclusions in the dementia brain 1 hippocampus (3221). Within the dementia brain 1 hippocampus the load of amyloid plaques (1439) is less than the load of *Cpn* inclusions (3221). Whereas within the dementia brain 1 prefrontal cortex the load of amyloid plaques (4965) is greater than the load of *Cpn* inclusions (3221).

For the dementia brain 2 the load of amyloid plaques in the prefrontal cortex (2608) is greater than the load of amyloid plaques in the hippocampus (1670). The load of *Cpn* inclusions in the dementia brain 2 prefrontal cortex (1263) is less than the load of *Cpn* inclusions in the dementia brain 2 hippocampus (1516). Within the dementia brain 2 prefrontal cortex the load of amyloid plaques (2608) is greater than the load of *Cpn* inclusions (1263). Within the dementia brain 2 hippocampus the load of amyloid plaques (1670) is greater than the load of *Cpn* inclusions (1516).

DISCUSSION

5.1 Amyloid Pathology and Characteristics

Amyloid plaque and *Cpn* immunoreactivity were observed in both the AD/dementia and non-AD/dementia brains. Notably, the morphology of amyloid plaques

varied between the AD/dementia and non/AD dementia brains as well as between the hippocampus and prefrontal cortex sections. Amyloid plaques are known to occur in a range of morphologies (Dickinson & Vickers, 2001, Thal et al. 2006), thus this variation is not indicative of any error in the immunolabeling or quantification procedure. Previous studies on the formation and progression of amyloid plaques in AD and other amyloidopathies have proposed a three-tiered morphology classification system which represents progressive stages of plaque maturation (Rohr et al, 2020; Ji,et al, 2018; Tagliavini et al, 1988). Under this system, the least mature amyloid plaque is referred to as diffuse, followed by compact, and finally the mature dense core plaque. Diffuse plaques can be identified by their thin, amorphous, cloud-like appearance and lack of clear borders or identifiable center point. Compact plaques appear uniformly dense, have well defined borders, and are likely to appear circular or ovoid in shape. Dense core plaques are identified by the presence of a particularly dense center point which is surrounded by a halo of distinctly less dense but still well-defined immunolabeling. These plaques are also usually circular or ovoid in shape.

The amyloid plaques found within the AD/dementia brains were overwhelmingly of the diffuse and compact type. The load of plaques in the prefrontal cortex of the AD/dementia brains noticeably skewed toward compact plaques, while the hippocampus was more likely to show an equal distribution of diffuse and compact amyloid plaques. Dense core plaques were still present in the AD/dementia brains, but at a dramatically lower rate than the other two morphologies. Additionally, dense core plaques were more likely to be found in the hippocampus of the AD/dementia brains than in the prefrontal cortex. The non-AD/dementia brain primarily contained compact and dense core amyloid plaques. Unlike the AD/dementia brains, in which all three plaque morphologies were

present to some degree, the non-AD/dementia brains showed little to no diffuse amyloid plaque morphology in either brain section. The hippocampus of the non-AD/dementia brains primarily showed dense core plaques with the occasional presence of compact plaques. Whereas the prefrontal cortex of the non-AD/dementia brains primarily showed compact plaques and few dense core plaques. In general, the hippocampus is more likely to contain dense core plaques and the prefrontal cortex is more likely to contain compact plaques. It should also be noted that although dense core plaques were identified as one of the primary plaque morphologies observed in the non-AD/dementia brains, this does not indicate that the non-AD/dementia brains contain more dense core plaques than the AD/dementia brains. This description simply indicates that of the plaques that were observed in the non-AD/dementia brains, many were dense cored. Furthermore, considering the greater total load of amyloid plaques found in AD/dementia brains compared to the non-AD/dementia brains, it is highly likely that the AD/dementia brains contain more dense core plaques than the non-AD/dementia brains.

Each of the three plaque morphologies are associated with a specific biochemical composition (Thal et al. 2006, Rohr et al. 2020). Diffuse plaques are primarily composed of low concentrations of oligomeric and protofibrillar Aβ42. Compact plaques are primarily composed of high concentrations of oligomeric and protofibrillar Aβ42 as well as varying levels of mature Aβ42 fibrils. The core of a dense core plaque is composed of tightly packed mature Aβ42 fibrils while the halo is composed of low concentration of oligomeric and protofibrillar Aβ42 similar to that of the diffuse plaques (Rohr et al. 2020). This change in amyloid plaque makeup observed from diffuse to dense primarily validates the notion that each category represents progressive stages of plaque maturation (Rohr et al. 2020). However, the specific makeup that characterizes each plaque

morphology additionally has interesting implications for the pathology of AD. As mentioned previously, the Aβ42 mature fibrils and the Aβ42 oligomers are known to exert a cytotoxic effect. However, the Aβ42 oligomers are considered the main cause of the neurotoxic damage seen in AD (Tamango et al, 2018; Verma et al, 2015). Thus, it is possible that a greater load of diffuse and compact plaques represents greater neurotoxic stress on the brain. This assumption would follow from the IHC results of this study which demonstrated that AD/dementia brains carry a high load of both diffuse and compact plaques, and thus a high load of the neurotoxic Aβ42 oligomer. Furthermore, as diffuse and compact plaques likely represent less mature and thus more recently formed amyloid plaques, it is possible that an abundance of these plaque morphologies represent a rapid rate of new plaque formation as might be expected from the positive feedback loop of plaque formation caused by secondary nucleation likely to occur in later stage AD (Verma et al, 2015)

5.2. Cpn pathology and morphology

Immunolabeling for the presence of *Cpn* revealed two patterns of *Cpn* immunoreactivity. The first pattern of *Cpn* immunoreactivity were punctate inclusions. This pattern represented the majority of inclusions observed in every brain where *Cpn* was present. Previous research has suggested that these punctate inclusions are indicative of the elementary body phase of the *Cpn* lifecycle (Hammond et al, 2010; Hybiske & Stevens, 2007). The second pattern of *Cpn* immunoreactivity were larger cloud-like inclusions. These inclusions were significantly less common than the punctate elementary bodies and occurred primarily in the AD/dementia brains. The hippocampus and prefrontal cortex of the AD/dementia brains did not display a noticeable difference in the frequency of these cloud-like inclusions. Previous research has suggested that these

inclusions represent factors such as lipopolysaccharides that have been secreted by *Cpn* (Hammond, 2010; Hybiske & Stevens, 2007), however no literature was found that has associated this labeling pattern with a particular life cycle phase or specific behavior of *Cpn*. As these cloud-like inclusions primarily occurred in the AD/dementia brains it is possible that this labeling pattern is indicative of a more active *Cpn* infection. For example, like many obligate intracellular bacteria, *Cpn* relies on the secretion of effector proteins, such as CPn0572, CPn0677, and CPn0678, to prime the host cell membrane for entry (Hansch, 2020). The cloud of immunoreactivity may represent these secreted effector proteins, and thus show a *Cpn* bacterium in the process of entering a new host cell.

5.3 Amyloid Plaques and *Cpn* Inclusion Counts

The primary questions investigated by this study were, firstly, if amyloid plaque load correlates with *Cpn* inclusion load, and secondly, if there is a difference in amyloid plaque and *Cpn* inclusion load between AD/dementia and non-AD/dementia brains. It has been well established in the literature that AD is associated with an increased load of amyloid plaques (Barage et al, 2015). Additionally, previous research regarding the relationship between AD and *Cpn* has suggested that AD status is correlated with the presence of *Cpn* (Balin et al, 1998; Bu et al, 2015; Contini et al, 2010; Ecemis et al, 2010; Hammond et al, 2010; Itzhaki et al, 2004; Little et al, 2004; Little et al, 2014; Lim et al, 2014). Thus, it follows that the load of *Cpn* inclusions likely positively correlates with the load of amyloid plaques and furthermore the load of amyloid plaques and *Cpn* inclusions will be greater in the AD/dementia brains than in the non-AD/dementia brains. The total counts recorded in this study confirm these assumptions. The results showed a strong positive correlation between the load of amyloid plaques and *Cpn* inclusions, regardless

of AD/dementia or non-AD/dementia status. Additionally, the load of amyloid plaques and *Cpn* inclusions was substantially higher in the AD/dementia brains for both sections compared to the non-AD/dementia brains.

The total counts additionally revealed an interesting relationship between the load of amyloid plaques and *Cpn* inclusions within the hippocampus and prefrontal cortex which was independent of AD/dementia or non-AD/dementia status. The prefrontal cortex of both the AD/dementia and non-AD/dementia brains displayed a higher load of amyloid plaques than *Cpn* inclusions. The difference between the load of amyloid plaques and *Cpn* inclusions was substantial, with AD/dementia prefrontal cortex showing 2.07x more amyloid plaques than *Cpn* and the non-AD prefrontal cortex showing 2.23x more amyloid plaques than *Cpn*. The hippocampus on the other hand shows a greater load of *Cpn* than amyloid plaques. The difference between the load of amyloid plaques and *Cpn* inclusions in the hippocampus was not as extreme as in the prefrontal cortex. The AD/dementia hippocampus showed 1.23x more *Cpn* inclusions than amyloid plaques while the non-AD/dementia hippocampus showed 1.26x more *Cpn* inclusions than amyloid plaques. However, there is significant overlap in the standard error between the *Cpn* inclusion counts and amyloid plaques counts in the non-AD/dementia hippocampus so the difference within the non-AD/dementia hippocampus may not be meaningful. The consistent relationship between the relative loads of amyloid plaque and *Cpn* inclusions across AD/dementia and non-AD/dementia brain structures is potentially vital evidence towards the infection hypothesis of AD, as it demonstrates that *Cpn* may be present from the earliest stages of AD. This reduces the likelihood that the increased presence of *Cpn* observed in this, and previous studies is the result of a third variable, such as a

compromised CNS immunity or a damaged blood brain barrier which may occur in the later stages of AD.

5.4 Conclusion

This study was the first to quantify an infection with *Chlamydia pneumoniae* and production of amyloid plaques. The hypothesis underlying this study is that load of *Chlamydia pneumoniae* correlates with degree of amyloid pathology within the limbic system. The results provide strong evidence demonstrating this correlation. The load of *Cpn* consistently correlated with load of amyloid plaques in the regions of the brain anaylzed. Additionally, the load of both amyloid plaques and *Cpn* was markedly higher in the brains where AD/dementia was recorded on the death certificate compared to the brains where a COD other than AD/dementia was recorded. Prior research has suggested that *Cpn* may act as trigger for the formation of amyloid plaques through the initiation of an inflammatory response (Al-Atrache et al., 2019, Lim et al, 2014; Little et al, 2014; Little et al, 2004; Hammond et al, 2006; Ou et al, 2021). While the results of this study cannot confirm whether this is indeed the case, nor can this study even claim a causal relationship between infection and AD/dementia, the results further validate the findings of these previous studies by demonstrating the connection between *Cpn* and amyloid in humans with AD/dementia diagnoses.

Previous research has also suggested that *Cpn* enters the CNS via an olfactory route of infection (Little et al, 2014; Little et al, 2005; Itzhaki et al, 2004). The body of work demonstrating this connection was a primary motivator for specifically investigating the limbic system for *Cpn* and AD pathology. Unlike other afferent pathways which first synapse at the thalamus, the olfactory nerve synapses directly to the

limbic system. Thus, assuming that *Cpn* is a possible trigger for the formation of amyloid plaques and assuming that *Cpn* enters the CNS via the olfactory pathway then the olfactory blub and related limbic structures should be among the first areas to show AD pathology. This is indeed the case, with the earliest neural damage in LOAD occurring in the lateral entorhinal cortex followed by damage in the hippocampal formation (Christen-Zaech et al, 2003; Mann et al 1988; Balin & Hudson, 2020). The result of this study may also serve to validate these findings. Firstly, the hippocampus of both the AD/dementia and non-AD/dementia brains revealed a higher frequency of amyloid plaques of mature morphology compared to the corresponding prefrontal cortices. Within the AD/dementia brain, amyloid plaques of compact morphology predominated alongside a less common but still appreciable presence of dense core plaques. The non-AD/dementia hippocampus meanwhile displayed primarily dense core plaques alongside some compact plaques. This difference in morphology may possibly provide evidence that plaques have been forming in the hippocampus for a longer period of time than in the prefrontal cortex, and thus that *Cpn* may have been present for longer. Secondly, the load of *Cpn* inclusions found within the AD/dementia hippocampus was greater than the load found with the prefrontal cortex. This again may be evidence that within these brain *Cpn* infection occurs in the hippocampus earlier than in the prefrontal cortex.

This study additionally serves to validate the use of the Human Gifts Registry (HGR) as a viable and useful source of experimental tissue. The HGR is non-profit agency of the Commonwealth of Pennsylvania concerned primarily with the donation and distribution of bodies to all medical and dental schools in the state for research and teaching purposes (Human Gifts Registry, 2022). As the HGR donates whole cadavers to institutions, it provides researchers with a high degree of control and flexibility. For

example, every brain used in this study was harvested from cadavers donated by the HGR. As such, this allowed the researchers to oversee nearly every step of the experimental process, from dissection to formalin fixation, and paraffin embedding. Furthermore, as the entire brain was on hand and accessible to the researchers, changes or additions to the experiment could be implemented with ease and at the researcher's convenience. However, most vitally, this study demonstrated that the diagnostic information provided by HGR on the donor is accurate enough to use in experimentation. The only information provided by HGR regarding the cadavers is age, gender, race, and COD. No further medical records or history are provided. Thus, this experiment relied entirely on COD to create the AD/dementia and non-AD/dementia groups. Since the results of this study showed a substantially higher load of amyloid plaques in the AD/dementia brains compared to the non-AD/dementia brains the COD provided by the HGR for each brain was likely accurate as a COD.

REFERENCES

Al-Atrache, Z., Lopez, D. B., Hingly, S. T., Appelt, D. M. (2019). Astrocytes infected with Chlamydia pneumoniae demonstrate altered expression and activity of secretases involved in the generation of β-amyloid found in Alzheimer disease. BMC Neurosci, 20(6). https://doi.org/10.1186/s12868-019-0489-5

Appelt, D. M. & Balin, B.J (1993). Analysis of Paired Helical Filaments Found in Alzheimer Disease Using Freeze-Drying/Rotary Shadowing. J. Struct. Biol. 111: 85-95.

Balin, B. J., Gerard H. C., Arking E. J., Appelt D. M., Branigan P. J., Abrams J. T., et al (1998). Identification and localization of Chlamydia pneumoniae in the Alzheimer's brain. Med Microbiol Immunol, 187, 23–42.

Balin, B. J., Hammond, C. J., Little, C. S., Hingley, S. T., Al-Atrache, Z., Appelt, D. M. (2018) Wittum-Hudson, J. A., Hudson, A. P. (2018). Chlamydia pneumoniae: An Etiologic Agent for Late-Onset Dementia. Frontiers in Agining Neuroscience, 10(302). https://doi.org/10.3389/fnagi.2018.00302

Balin, B. J. & Hudson, A. P. (2020). Perspectives on the Intracellular Bacterium Chlamydia pneumoniae in Late-Onset Dementia. Cuurent Clinical Microbiology Reports, 2020(7), 90-99. https://doi.org/10.1007/s40588-020-00146-4

Barage, S. H. & Sonawane, K. D. (2015). Amyloid cascade hypothesis: Pathogenesis and therapeutic strategies in Alzheimer's disease. Neuropeptides, 52(2015), 1-18. http://dx.doi.org/10.1016/j.npep.2015.06.008

Bertram L., Lill C. M., Tanzi R. E. (2010) The genetics of Alzheimer disease: back to the future. Neuron, 68(2), 270–281. doi: 10.1016/j.neuron.2010.10.013.

Bu, X.L., Yao, X.Q., Jiao, S.S., Zeng, F., Liu, Y.H. et al (2015). A study on the association between infectious burden and Alzheimer's disease. Eur. J. Neurol, 22, 1519–1525.

Carrero, I., Gonzalo, M. R., Martin, B., Sanz-Anquela, J. M., Arevalo-Serrano, J., Gonzalo-Ruiz, A. (2012). Oligomers of beta-amyloid protein (Aβ1-42) induce the activation ofcyclooxygenase-2 in astrocytes via an interaction with interleukin-1beta, tumournecrosis factor-alpha, and a nuclear factor kappa-B mechanism in the rat brain. Experimental Neurology, 236, 215-227. http://dx.doi.org/10.1016/j.expneurol.2012.05.004

Christen-Zaech S, Kraftsik R, Pillevuit O, Kiraly M, Martins R, Khalili K, et al. (2003). Early olfactory involvement in Alzheimer's disease. Can J Neurol Sci, 30(1), 20–5

Contini, C., Seraceni, S., Cultrera, R., Castellazzi, M., Granieri, E., Fainardi, E. (2010). Chlamydophila pneumoniae Infection and Its Role in cognitive impairment through enhancement of beta-amyloid. Neurological Disorders, 2010. doi:10.1155/2010/273573

Cummings, J. (2021). Drug Development for Psychotropic, Cognitive-Enhancing, and Disease-Modifying Treatments for Alzheimer's Disease. J. Neuropsychiatry Clin Neurosci, 33(1), 3–13, doi: 10.1176/appi.neuropsych.20060152

Deniset, J.F., Cheung, P.K.M., Dibov, E., Lee, K., Stiegerwald, S., Pierce, G.N. (2010) *Chlamydophila pneumoniae* Infection Leads to Smooth Muscle Cell Proliferation and Thickening in the Coronary Artery without Contributions from a Host Immune Response**.** The American Journal of Pathology, 176(2), 1028-1037. https://doi.org/10.2353/ajpath.2010.090645

Dheen, S. T., Kaur, C., Ling, E. A. (2007). Microglial activation and its implications in the brain diseases. Current Medicinal Chemistry, 14(11), 1189-1197. https://doi.org/10.2174/092986707780597961

Dickenson T.C. & Vickers, J.C (2001). The morphological phenotype of β-amyloid plaques and associated neuritic changes in Alzheimer's disease, 105(1), 99-107. https://doi.org/10.1016/S0306-4522(01)00169-5

Di Sabato, D., Quan, N., Godbout, J. P. (2017). Neuroinflammation: The Devil is in the Details. J Neurochem, 139(Suppl 2), 136-153. doi: 10.1111/jnc.13607

Ecemis, T., Mavioglu, H., Ozkutuk, N., Akcali, S., Karacam, M., Sanlidag, T., (2010). Seroprevalance of Chlamydophila pneumoniae in patients with Alzheimer's disease and vascular dementia. J Neurol Sci Turk, 27, 400–406.

Garbuz, D. G., Zatsepina, O. G. & Evgen'ev, M. B. (2021). Beta Amyloid, Tau Protein, and Neuroinflammation: An Attempt to Integrate Different Hypotheses of Alzheimer's Disease Pathogenesis. Molecular Biology, 55(5), 734-747. doi: 10.1134/S002689332104004X

Gasparini, L., Rusconi, L., Xu, H., del Soldato, P., Ognini, E. (2004). Modulation of beta-amyloid metabolism by non-steroidal anti-inflammatory drugs in neuronal cell cultures. J. Neurochem, 88(2), 337-348. doi: 10.1111/j.1471-4159.2004.02154.x.

Gerard, H.C., Dreses-Werringloer, U., Wildt, K.S., Deka, S., Oszust, C., Balin, B.J., Frey 2nd, W.H., Bordayo, E.Z., Whittum-Hudson, J.A., Hudson, A.P., (2006). Chlamydophila (Chlamydia) pneumoniae in the Alzheimer's brain. FEMS Immunol. Med. Microbiol. 48, 355–366.

Goate A. & Hardy J. (2012). Twenty years of Alzheimer's disease-causing mutations. J Neurochem, 120(Suppl. 1), 3–8. doi: 10.1111/j.1471-4159.2011.07575.x.

Gonneaud, J., Baria, A. T., Binette, A. P. et al (2021). Accelerated functional brain aging in pre-clinical familial Alzheimer's disease. Nature Communications, 12(5346). https://doi.org/10.1038/s41467-021-25492

Gonzalez-Reyes, R. E., Nava-Mesa, M. O., Vargas-Sanchez, K., Ariza-Salamanca, D., Mora-Munoz, L. (2017). Involvement of Astrocytes in Alzheimer's Disease from a Neuroinflammatory and Oxidative Stress Perspective. Front Mol Neurosci, 10(427). doi: 10.3389/fnmol.2017.00427

Guerchet, M, Prince, M, Prina, M (2020, November 20). An update to the estimates in the World Alzheimer Report 2015. Alzheimer's Disease International. https://www.alzint.org/resource/numbers-of-people-with-dementia-worldwide/

Guerrero, A., De Strooper, B. & Arancibia-Carcamo, I. L. (2021). Cellular senescence at the crossroads of inflammation and Alzheimer's disease. Trends in Neuroscience, 44(9), 714-727. https://doi.org/10.1016/j.tins.2021.06.007

Guo, Y., Wang, Q., Chen, S., Xu, C., (2020). Functions of amyloid precursor protein in metabolic diseases. Metabolism Clinical and Experimental, 115(2021). https://doi.org/101.1015/j.metabol.2020.154454

Hammond, C. J., Hallock, L. R., Howanski, R. J., Appelt, D. M., Little, C. S., Balin, B. J. (2010). Immunohistological detection of Chlamydia pneumoniae in the Alzheimer's disease brain. BMC Neuroscience, 11(121). doi:10.1186/1471-2202-11-121

Hansch, S., Spona, D., Murra, G., Hegemann, J.H. (2020) Chlamydia-induced curvurture of the host cell plasma membrane is required or infection. PNAS, 117(5), 2634-2644. https://doi.org/10/1073/pnas.1911528117

Herrera-Landero, A., Amya-Sanchez, L.E., de Las-Deses, C.D.H., Solorzano-Santos, F., Gordillo-Perez, M.G. (2019). Borrelia burgdorferi as a risk factor for Alzheimer's dementia and mild cognitive impairment. Eur Geriatr Med 2019 Jun;10(3):493-500. doi: 10.1007/s41999-018-0153-0.

Human Gifts Registry (2022). Our Role. http://www.hgrpa.org/

Hybiske K, Stephens RS. Mechanisms of host cell exit by the intracellular bacterium Chlamydia. Proc Natl Acad Sci U S A. 2007 Jul 3;104(27):11430-5. doi: 10.1073/pnas.0703218104. Epub 2007 Jun 25. PMID: 17592133; PMCID: PMC2040915

Itzhaki, R.F., Wozniak, M.A., Appelt, D.M., Balin, B.J. (2004). Inflitration of the brain by pathogens causes Alzheimer's disease. Neurobiology of Aging, 25, 619-627. doi:10.1016/j.neurobiolaging.2003.12.021

Ji M, Arbel M, Zhang L, Freudiger CW, Hou SS, Lin D et al (2018) Label free imaging of amyloid plaques in Alzheimer's disease with stimulated raman scattering microscopy. Sci Adv 4:1–9. https://doi.org/10.1126/sciadv.aat7715

Jouanne, M., Rault, S., Volsin-Chiret, A-S (2017). Tau protein aggregation in Alzheimer's disease: and Attractive target for the development of novel therapeutic agents. European Journal of Medicinal Chemistry, 139, 153-167. http://dx.doi.org/10.1016/j.ejmerch.2017.07.070

Kern, J.M., Maass, V., Maass, M. (2009). Molecular pathogenesis of chronic *Chlamydia pneumoniae* infection: a brief overview. Clinical Microbiology and Infection, 15(1), 36-41. https://doi.org/10.1111/j.1469-0691.2008.02631.x

Khodamorandi, S., Shahhosseini, M.H., Mohammadian, T., Ferdousi, A. (2021). Evaluation of Role of Herpes Simplex Virus Types 1 and 2 and Cytomegalovirus in Alzheimer's Disease. Medical Laboratory Journal. DOI: 10.29252/mlj.15.4.39

Lee, K.H., Kwon, D.E., Kyung, D.H., La, Y., Han, S.H. Association between cytomegalovirus disease and dementia: A population-based cohort study. Research Square. https://doi.org/10.21203/rs.2.19035/v1

Lee, J. W., Lee, Y. K., Yuk, D. Y., Choi, D. Y., Ban, S. B., Oh, K. W., Hong, J. T. (2008). Neuro-inflammation induced by lipopolysaccharide causes cognitive impairment through enhancement of beta-amyloid generation. Journal of Neuroinflammation, 5(37). doi:10.1186/1742-2094-5-3

Lim C., Hammond C. J., Hingley S. T., Balin B. J. (2014) Chlamydia pneumoniae infection of monocytes in vitro stimulates innate and adaptive immune responses relevant to those in Alzheimer's Disease. J Neuroinflamm., 11(217)

Little, S.C., Hammond, C.J., Macintyre, A., Balin, B.J., Appelt, D.M. (2004) Chlamydia pneumoniae induces Alzheimer-like amyloid plaques in brains of BALB/c mice. Neurobiol Aging, 25(4), 419-29. doi: 10.1016/S0197-4580(03)00127-1

Little, S.C., Joyce, T.A., Hammond, C., Matta, H., Cahn, D. Et al (2014). Detection of Bacterial Antigens and Alzheimer's Disease-like Pathology in the Central Nervous System of BALB/c Mice Following Intranasal Infection with a Laboratory Isolate of Chlamydia pneumoniae. Front Aging Neurosci,6. doi: 10.3389/fnagi.2014.00304

Loeb, M.B., Molloy, D.W., Smieja, M., Standish, T., Goldsmith, C.H., Mahony, J., Smith, S., Borrie, M., Decoteau, E., Davidson, W., McDougall, A., Gnarpe, J., O'D, O.M., Chernesky, M. (2004). A randomized, controlled trial of doxycycline and rifampin for patients with Alzheimer's disease. J. Am. Geriatr. Soc., 52, 381–387.

Mahony, J.B., Woulfe, J., Munoz, D., Browning, D., Chong, S., Smieja, M., (2000). Identification of chlamydia pneumoniae in the Alzheimer's brain. Neurobiol. Aging, 21, 245.

Mann DM, Tucker CM, Yates PO. Alzheimer's disease: an olfactory connection? (1988) Mech Ageing Dev., 42(1), 1–15.

Mielcarska, M.B., Skowronska, K., Wyzewski, Z., Toka, F.N. (2022). Disrupting Neurons and Glial Cells Oneness in the Brain—The Possible Causal Role of Herpes Simplex Virus Type 1 (HSV-1) in Alzheimer's Disease. Int. J. Mol. Sci. 2022,23,242. https://doi.org/ 10.3390/ijms23010242

Millington, C., Sonego, S., Karunaweera, N., Rangel, A., Aldrich-Wight, J. R, Campbell, I. L., Gyengesi, E., Munch, G. (2014). Chronic Neuroinflammation in Alzheimer's Disease: New Perspectives on Animal Models and Promising Candidate Drugs. BioMed. Res. Int., 2014. http://dx.doi.org/10.1155/2014/309129

Morris, M., Maeda, S., Vossel, K., Mucke, L. (2011) The Many Faces of Tau. Neuron Review, 70, 410-426. doi: 10.1016/j.neuron.2011.0

Mucke, L., Selkoe, D.J. (2012). Neurotoxicity of Amyloid β-protein: Synaptic and Network Dysfunction. Cold Spring Harbor Perspective in Medicine, 12(2). doi: 10.1101/cshperspective.a006338

Muller, U.C., Deller, T., Korte., M. (2017). Not just amyloid: physiological functions of the amyloid precursor protein family. Nature Reviews: Neuroscience, 18, 281-298. doi:10.103b/nrn.2017.29

Naseri, N.N., Wang, H., Guo, J., Sharma, M., Luo, W. (2019). The complexity of Alzheimer's Disease. Neuroscience Letters, 705, 183-194. https://doi.org/10.1016/j.neulet.2019.04.022

Nochlin, D., Shaw, C.M., Campbell, L.A., Kuo, C.C., (1999). Failure to detect Chlamydia pneumoniae in brain tissues of Alzheimer's disease. Neurology, 53(1888).

Richard J O'Brien and Philip C. Wong (2011) Amyloid precursor protein processing and Alzheimer's disease, Annu Rev Neurosci. 2011; 34:185-204. doi: 10.1146/annurev-neuro-061010-113613

O'Brien, R.J., Wong, P.C. (2011). Amyloid precursor protein processing and Alzheimer's disease. Annual Review Neuroscience, 34, 185-204. doi: 10.1146/annurev-neuro-061010-113613

Ou, H., Chien, W-C., Chung, C-H, Chang, H-A., Kao, Y-C., Wu, P-C, Tzeng, N-S. (2021). Association Between Antibiotic Treatment of Chlamydia pneumoniae and Reduced Risk of Alzheimer Dementia: A Nationwide Cohort Study in Taiwan. Front. Aging Neurosci,13. doi: 10.3389/fnagi.2021.701899

Paradowski, B., Jaremko, M., Dobosz, T., Leszek, J., Noga, L., (2007). Evaluation of CSF Chlamydia pneumoniae, CSF-tau, and CSF-Abeta42 in Alzheimer's disease and vascular dementia. J. Neurol, 254, 154–159.

Parker, K. & Rhee, Y. (2020). Alzheimer's Disease Warning Signs: Gender and Education Influence Modifiable Risk Factors—A Pilot Survey Study. Journal of the American College of Nutrition, 40(7), 585-588. https://doi.org/10.1080/07315724.2020.1812451

Qiu, T., Liu, Q., Chen, Y-X., Zhao, Y-F., Li, M-Y. (2015). Aβ42 and Aβ40: similarities and differences. Journal of Peptide Science, 21, 522-529. doi: 10.1002/psc.2789

Ring, R.H. & Lyons, J.M., (2000). Failure to detect Chlamydia pneumoniae in the late-onset Alzheimer's brain. J. Clin. Microbiol, 38, 2591–2594.

Rohr, D., Boon, D.D.C, Schuler, M., Kremer, K. et. Al (2020). Label-free vibrational imaging of different Aβ plaque types in Alzheimer's disease reveals sequential events in plaque development. Acta Neuropathologica Communications, 8(22). https://doi.org/10.1186/s40478-202-01901-5

Senejani, A.G., Maghsoudlou, J., El-Zohiry, D., Gaur, G. Et al. (2021). Borrelia burgdorferi Co-Localizing with Amyloid Markers in Alzheimer's Disease Brain Tissues. Journal of Alzheimer's Disease, 85, 889–903. DOI 10.3233/JAD-215398

Steiner, H., Fukumori, A., Tagami, S., Okochi, M. (2018) Making the final cut: pathogenic amyloid-β peptide generation by γ-secretase. Cell Stress, 2(11), 292-310. doi: 10.15698/cst2018.11.162

Tagliavini F, Giaccone G, Frangione B, Bugiani O (1988) Preamyloid deposits in the cerebral cortex of patients with Alzheimer's disease and nondemented individuals. Neurosci Lett 93, 191–196. https://doi. org/10.1016/0304-3940(88)90080-8

Tamangno, E., Guglielmotto, M., Monteleone, D., Manassero, G., Manassero, G., Vasciaveo, V., Tabaton, M. (2018). The unexpected role of Aβ1-42 monomers in the pathogenesis of Alzheimer's disease. Journal of Alzheimer's Disease, 62, 1241-1245. doi: 10.3233/JAD-170581

Taylor, G.S., Vipond, I.B., Paul, I.D., Matthews, S., Wilcock, G.K., Caul, E.O. (2002). Failure to correlate C. pneumoniae with late onset Alzheimer's disease. Neurology, 59, 142–143.

Terrando, N., Fidalgo, A.R., Vizcaychipi, M., Cibelli, M., Ma, D., Monaco, C., Feldmann, M. & Maze, M. (2010) The impact of IL-1 modulation on the development of lipopolysaccharide-induced cognitive dysfunction. Critical Care, 14(R88). doi: 10.1186/cc9019

Thal D.R., Capetillo-Zarate, E., Del Tredici, K., Braak, H. (2006). The development of amyloid-β protein deposits in the aged brain. Sci. Aging Knowl. Environ, 6. doi: 10.1126/sageke.2006.6.re1

Verma, M., Vats, A., Taneja, V. (2015). Toxic species in amyloid disorders: Oligomers or mature fibrils. Annals of Indian Academic Neurology, 18(2), 138-145.

Wang A., Al'Kuhlani M., Johnston S. C., Ojcius D. M., Chou J., Dean D. (2013). Transcription factor complex AP-1 mediates inflammation initiated by Chlamydia pneumoniae infection. Cell Microbiol., 15, 779-794.

Wang, J-Z., Xia, Y-Y., Grundke-Iqbal, I., Iqbal, K. (2013). Abnormal hyperphosphorylation of tau: Sites, regulation, and molecular mechanics of neurofibrillary degeneration. Journal of Alzheimer's Disease, 33, S123-S139. doi: 10.3233/JAD-2012-129031

Wegmann, S., Biernat, J. & Mandelkow, E. (2021). A current view on Tau protein phosphorylation in Alzheimer's disease. Current Opinion in Neurobiology, 69(131), 131-138. https://doi.org/10.1016/j.conb.2021.03.003

Wilkins, H.M & Swerdlow, R.H (2017). Amyloid precursor protein processing and bioenergetics. Brain Research Bulletin, 133(2017), 71-79. http://doi.org/10.1016/j.brainresbull.2016.08.009

Wilquet, V., De Strooper, B. (2004). Amyloid-beta precursor protein processing in neurodegeneration. Current Opinion in Neurobiology, 14, 582-588. doi: 10.1016/j.conb.2004.08.001.

Woods, J. J., Skelding, K. A., Martin, K. L., Aryal, R., Sontag, E., Johnstone, D. M., Horvat, J. C., Hansbro, P. M., Milwad, E. A. (2020). Assessment of evidence for or against contributions of Chlamydia pneumoniae T infections to Alzheimer's disease etiology. Brain, Behavior, and Immunity, 83(2020), 22-32. https://doi.org/10.1016/j.bbi.2019.10.014

Wozniak, M.A, Mee, A.P, Itzhaki, R.F. (2009). Herpes simplex virus type 1 DNA is located within Alzheimer's disease amyloid plaques. J Pathol 2009; 217: 131–138. DOI: 10.1002/path.2449

Yamamoto, H., Watanabe, T., Miyazaki, A., Katagiri, T., Idei, T., Iguchi, T., Mimura, M., Kamijima, K. (2005). High prevalence of Chlamydia pneumoniae antibodies and in- creased high-sensitive C-reactive protein in patients with vascular dementia. J. Am. Geriatr. Soc., 53, 583–589.

Zhang, F., Gannon, M., Chen, Y., Yan, S., Zhang, S., Feng, W. et al (2020). β-amyloid redirects norepinephrine signaling to activate the pathogenic GSK3β/tau cascade. Sci Transl Med., 12(526). doi:10.1126/scitranslmed.aay6931.

Zhao, L.N., Long, H.W., Yuguang, M., Chew, L.Y. (2012) The Toxicity of Amyloid β Oligomers. International Journal of Molecular Science, 13(6), 7303-7327. https://doi.org/10.3390/ijms13067303

APPENDIX

If there is more than one appendix, label by letter (Appendix A, Appendix B, etc.).

Appendix material may be single-spaced and of a different font than the rest of the thesis.

Use “Normal” style for a single-spaced style, or “PCOM Thesis Body” for double space.